Modelling of Galfenol nanowires for Sensor Applications

A THESIS
SUBMITTED TO THE FACULTY OF THE GRADUATE SCHOOL
OF THE UNIVERSITY OF MINNESOTA
BY

KRISHNAN SHANKAR NARAYAN

IN PARTIAL FULFILLMENT OF THE REQUIREMENTS
FOR THE DEGREE OF
Master of Science

May, 2010

Acknowledgements

I would like to thank my advisor Professor Richard D James. He has been instrumental in introducing Mechanics to me and has been kind enough to let me freely decide the direction of my research. I would also like to thank Professor Roger Fosdick whose courses have been a great learning experience for me.

Dedication

Dedicated to my late father Shri V Krishnan and my neice Annapurna

Abstract

Galfenol is a new magnetostrictive material with potential applications in sensors for acoustic waves. The purpose of the present investigation is to study the properties of galfenol nanowires of nanometer range diameter relevant to sensing of acoustic waves using the phenomenon of magnetostriction. In this endeavor we study first the basic energetics for this material. Then we investigate the macro-scale behaviour for galfenol using the theory of "Large body limits in Ferro-magnetism" of Desimone [DS93]. Subsequently we look at the existence and stability of single domain states in galfenol nanowires. The theoretical predictions are then verified by numerical methods.

Contents

List of Tables

List of Figures

Chapter 1

Introduction

- Chapter 2 briefly describes properties of Galfenol and comparison with Terfenol.
- In Chapter 3 we describe the theoretical micromagnetic framework relevant to the physics of magentostriction. Within this framework we calculate the energy of typical configurations for Galfenol.
- Chapter 4 describes investigation of samples of Galfenol in millimeter size range. This involves calculation of natural frequencies of vibration for millimeter size beams. Later we use the "large body limit" model for ferromagnetism to compute virgin magnetization M vs H curves starting from ideal demagnetized state to magnetic saturation.
- Chapter 5 studies the existence of single domain state solutions for nanowires Galfenol samples and second-variation stability of these solutions. The stability and nucleation of bifurcation modes lead to a system of linear elliptic equations which are hard to solve for in closed form. We deal with this problem by proposing models for bifurcation solutions.
- Chapter 6 studies numerically the nucleation problem of the previous chapter and then compares the numerical results with theoretical results of previous chapter.

Chapter 2

Galfenol : New magnetostrictive material

Magnetostrictive solids are those in which reversible elastic deformations can be caused by changes in the magnetization. These materials have a coupling of typical ferromagnetic energies with elastic energies. Typically magnetostriction is a small effect in the range of 20-200 ppm for commonly occuring ferromagnetic materials like Fe, Co and Ni alloys. In the 1970's giant magnetostrictive alloys like $Tb_{0.3}Dy_{0.7}Fe_2$ were developed. This alloy called Terfenol has high magnetostriction of the order $\sim$ 2000 ppm but is very brittle and has low tensile strength of the order $\sim$ 100 MPa. For this reason in most sensor/actuator applications it is used under compressive strain. Recent research by Clark et.al. [CRWF$^+$00] has led to the development of a new alloy called "Galfenol" $Fe_{100-x}Ga_x$ where x ranges from $10\% - 30\%$. These alloys have high magnetostriction $\sim$ 400 ppm and high tensile strengths $\sim 400MPa$. While the exact physics of how gallium affects the magnetostriction is still being investigated, a lot of work has been done to study the $Fe_{100-x}Ga_x$ phase diagram and measure the magnetic properties of individual phases.

Fig 2.1 taken from [IKO$^+$02] shows the phase diagram for $Fe_{100-x}Ga_x$ alloys. The important phases related to magnetostriction property are the disordered A_2 or $\alpha\prime$ phase, the ordered B_2 or $\alpha\prime\prime$ phase which has a Cs-Cl structure and the ordered $D0_3$ phase. The magnetostriction as measured by $\frac{3}{2}\lambda_{100}$ has two peaks at 19% and 28% gallium

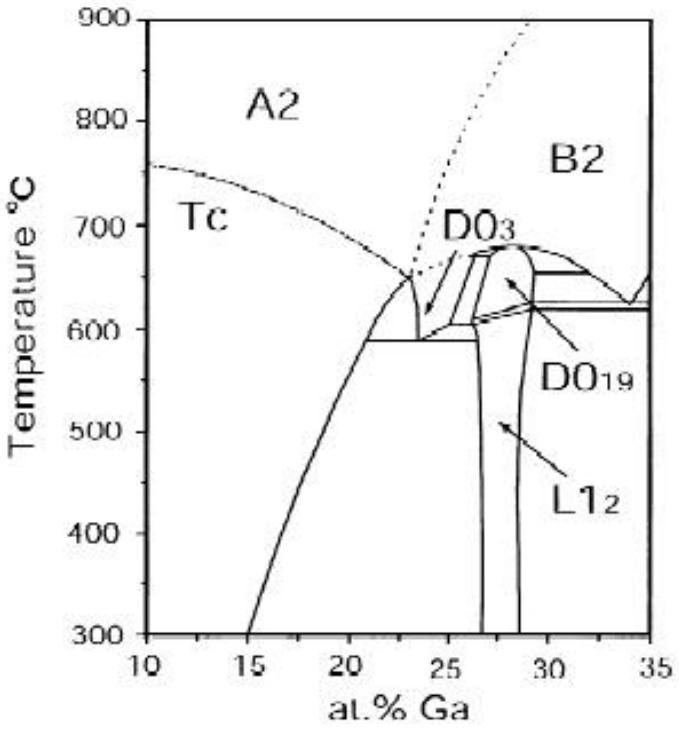

Figure 2.1: Phase-diagram

with approximate values of 400ppm and 450ppm [CHWF$^+$03] respectively.

The Table 2.1 shows a comparison of various physical properties of galfenol vs. terfenol which illustrates the basic problem with terfenol and the reason for development of galfenol. Data presented in this table is compiled from various references as [RCWC04], [PHL$^+$05], [CHWF$^+$03].

In recent years a lot of new experimental techniques have been developed to manufacture ferromagnetic wires of nanometer diameter e.g. electron-beam lithography, step growth and template-assisted electrodeposition. A possible application of these nanosize wires is in making acoustic sensors. The inspiration for this application comes from the structure of the human ear. Fig 2.3 shows a schematic of the inner ear. The inner ear has fine cilia like hair whose response to impinging acoustic waves is transmitted through the nervous system to the brain. One possible arrangement of galfenol

Table 2.1: Comparison of Magnetostrictive Data for Terfenol and Galfenol

Headings	Terfenol	Galfenol -18	Galfenol -28
Easy Axis	[111]	[100]	[100]
Elastic Modula			
c_{11} (GPa)	141	200	155
c_{12} (GPa)	65	220	210
c_{44} (GPa)	49	120	134
Anisotropy Constant $K_1(kJ/m^3)$	-60	30	-1
Magnetostriction $\frac{3}{2}\lambda$	1800	400	400
Staturation Magnetization M_s (Tesla)	1	1.6	1.15

nanowires is in the form of an array depicted in Fig 2.2. Here impinging acoustic waves are expected to induce a detectable change in the magnetization of the array.

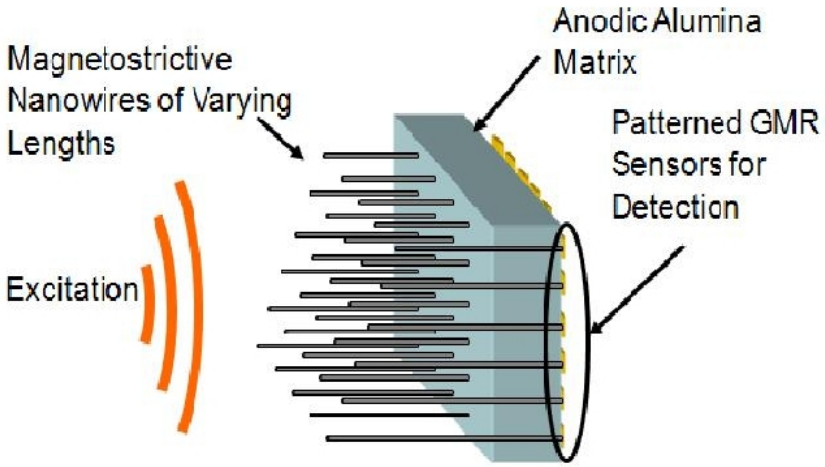

Figure 2.2: Proposed Sensor

The chief aim of this thesis is to conduct investigations into modeling nanometer size arrays of magnetostrictive materials for sensor application with a focus on galfenol.

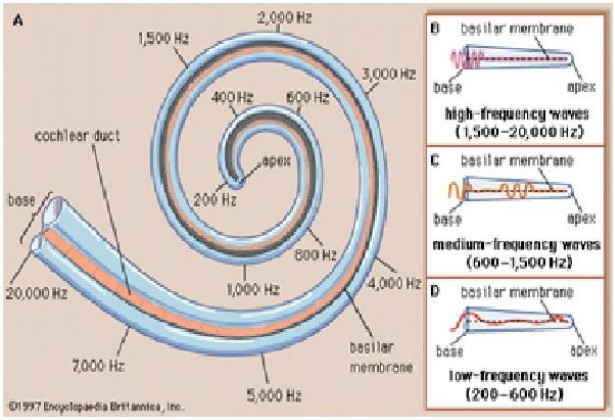

Figure 2.3: Inner ear

Chapter 3

Micromagnetic Energies

The initial model for ferromagnetic solids was proposed by Landau and Lifshitz(1935) [LL35]. The continuum theory of ferromagnetic materials was systematically developed in the works of Brown(1963) [Bro63] which was subsequently expanded to a theory for magnetostriction in Brown(1966) [Bro66], where a variational model for magnetostriction with small strain was developed. Henceforth in this investigation we will refer to the above framework developed in [Bro66] as Brown's model.

We now look at the energetics of magnetostriction using Brown's model for magnetostriction. Let Ω be a smooth reference configuration in $\mathbb{R}^3$. Let $\boldsymbol{m}(\boldsymbol{x})$ be the magnetization vector at some point $\boldsymbol{x} \in \Omega$. Below the Curie temperature, the magnetization is constrained to have constant euclidean norm i.e,

$$|\boldsymbol{m}(\boldsymbol{x})| = m_s \quad a.e. \qquad \boldsymbol{x} \in \Omega. \tag{3.1}$$

If Ω is a bounded domain, this constraint implies $\boldsymbol{m} \in L^p(\Omega, m_s S^2), \quad \forall 1 \leq p \leq \infty$. We extend $\boldsymbol{m}$ by 0 outside Ω whenever necessary and denote it in this work by $\boldsymbol{m}\chi_\Omega$ where obviously we have $\boldsymbol{m}\chi_\Omega \in L^p(\mathbb{R}^3, m_s S^2), \quad \forall 1 \leq p \leq \infty$. We denote by $\boldsymbol{y} : \Omega \mapsto \mathbb{R}^3$, the deformation map and the corresponding displacement by $\boldsymbol{u}(\boldsymbol{x}) = \boldsymbol{y}(\boldsymbol{x}) - \boldsymbol{x}$. The infinitesimal strain corresponding to displacement $\boldsymbol{u}(\boldsymbol{x})$ is given by,

$$\begin{aligned} \boldsymbol{E}(\boldsymbol{x}) &= \frac{1}{2}(\nabla \boldsymbol{y}(\boldsymbol{x}) + \nabla \boldsymbol{y}(\boldsymbol{x})^T) - \boldsymbol{I} \\ &= \frac{1}{2}(\nabla \boldsymbol{u}(\boldsymbol{x}) + \nabla \boldsymbol{u}(\boldsymbol{x})^T). \end{aligned} \tag{3.2}$$

Here the superscript T denotes the transpose operation over a matrix. It is assumed that $\boldsymbol{y} \in H^1(\Omega, \mathbb{R}^3)$. The magnetization vector in a magnetostrictive body causes a spontaneous local distortion of the lattice given by the map

$$\boldsymbol{m} \mapsto \boldsymbol{E}_0(\boldsymbol{m}) \in M^{3\times 3}_{\text{sym}},$$

where $M^{3\times 3}_{\text{sym}}$ denotes the set of symmetric matrices of 3×3 dimension. The tensor $\boldsymbol{E}_0$ is called the spontaneous or stress free strain.

Now we list the various energies which are part of the variational micromagnetics model for magnetoelastic solids.

3.1 Anisotropy Energy

The interaction of magnetic properties with crystalline structure of magnetic solids causes magnetic materials to have easy axis of magnetization. This phenomenon of having preferential directions of magnetization is modeled by a function, $\varphi : m_s S^2 \to [0, \infty)$. The most common types of anisotropy found in magnetic solids is usually uniaxial anisotropy and cubic anisotropy which occur in hexagonal and cubic crystal structures respectively. The energy has wells along a set of magnetization vectors $\{\boldsymbol{m}_k\}$. On these wells without loss of generality we can set $\varphi(\boldsymbol{m}_k) = 0$. The general form for φ for cubic materials is,

$$\varphi(\boldsymbol{m}) = \frac{K_1}{m_s^4}(m_x^2 m_y^2 + m_x^2 m_z^2 + m_y^2 m_z^2) + \frac{K_2}{m_s^6}(m_x^2 m_y^2 m_z^2).$$

Depending on the sign and magnitude of K_1 and K_2, the family of energy wells $\{\boldsymbol{m}_k\}$ could be oriented along the crystallographic families like $\langle 100\rangle, \langle 111\rangle$ etc. The anisotropy energy thus becomes,

$$E_{anis} = \int_\Omega \varphi(\boldsymbol{m})\, \boldsymbol{dx}.$$

3.2 Exchange Energy

The exchange energy penalizes variations in the magnetization in a body and thus tends to prefer constant magnetizations. It is modeled as follows,

$$E_{exc} = \frac{C}{2m_s^2} \int_\Omega |\nabla \boldsymbol{m}|^2\, \boldsymbol{dx}.$$

Here C is called the Exchange constant and the vector norm used is as follows,

$$|\nabla \boldsymbol{m}|^2 = |\nabla m_x|^2 + |\nabla m_y|^2 + |\nabla m_z|^2.$$

3.3 Demagnetization Energy

The demagnetization energy is the L^2 norm of the Helmholtz projection of the magnetization vector $\boldsymbol{m}\chi_\Omega \in L^2(\mathbb{R}^3, m_s S^2)$ on the gradient fields. The demagnetization field $\boldsymbol{h_m}$ is thus given by the following equation,

$$\nabla \cdot (-\nabla u(\boldsymbol{x}) + 4\pi \boldsymbol{m}(\boldsymbol{x})) = 0 \qquad \forall \boldsymbol{x} \in \mathbb{R}^3,$$

$$\boldsymbol{h_m}(\boldsymbol{x}) = -\nabla u(\boldsymbol{x}),$$

$$[|\nabla u \cdot \boldsymbol{n}|] = [|-\boldsymbol{h}_m \cdot \boldsymbol{n}|] = \boldsymbol{m} \cdot \boldsymbol{n}.$$

$[|\cdot|]$ represents the jump of a quantity across any oriented surface with unit normal $\boldsymbol{n}$. The demagnetization energy is thus given by,

$$E_m = \frac{1}{8\pi} \int_{\mathbb{R}^3} |\boldsymbol{h}_m(\boldsymbol{x})|^2 \, \boldsymbol{dx} = -\frac{1}{2} \int_\Omega \boldsymbol{h}_m(\boldsymbol{x}) \cdot \boldsymbol{m}(\boldsymbol{x}) \, \boldsymbol{dx}.$$

See appendix A for more on magnetostatic energy.

3.4 Zeeman Energy

The energy of interaction between an external applied field and the magnetization over the body is modeled by the following,

$$E_{app} = -\int_\Omega \boldsymbol{h}_a(\boldsymbol{x}) \cdot \boldsymbol{m}(\boldsymbol{x}) \, dx.$$

Here $\boldsymbol{h}_a$ is the applied field. In physical problems this term models a field applied by a electromagnet or permanent magnet such that the field $\boldsymbol{h}_a$ remains unchanged by any changes in the magnetization over the domain Ω.

3.5 Elastic Energy

The elastic energy for the magnetoelastic solid for small strains is given by,

$$E_{elastic} = \int_\Omega \frac{1}{2}(\boldsymbol{E}(\boldsymbol{x}) - \boldsymbol{E}_0(\boldsymbol{m})) \cdot \mathbb{C}[\boldsymbol{E}(\boldsymbol{x}) - \boldsymbol{E}_0(\boldsymbol{m})]\, \boldsymbol{dx}.$$

We recall $\boldsymbol{E}_0$ is the spontaneous strain induced by the magnetization $\boldsymbol{m}$ and $\boldsymbol{E}(\boldsymbol{x})$ is the strain corresponding to displacement $\boldsymbol{u}(\boldsymbol{x})$. For cubic materials its form is,

$$\boldsymbol{E}_0(\boldsymbol{m}) = \frac{3}{2}\begin{bmatrix} \lambda_{100}(\nu_x^2 - \frac{1}{3}) & \lambda_{111}\nu_x\nu_y & \lambda_{111}\nu_x\nu_z \\ \lambda_{111}\nu_y\nu_x & \frac{3}{2}\lambda_{100}(\nu_y^2 - \frac{1}{3}) & \lambda_{111}\nu_y\nu_z \\ \lambda_{111}\nu_z\nu_x & \lambda_{111}\nu_z\nu_y & \lambda_{100}(\nu_z^2 - \frac{1}{3}) \end{bmatrix}.$$

Here $\nu_i(\boldsymbol{x})$ are the direction cosines of the magnetization vector $\boldsymbol{m}(x)$, i.e. $\nu_i(\boldsymbol{x}) = \dfrac{m_i}{m_s}$, $i = x, y, z$. Thus the full energy functional for magnetostriction is,

$$\begin{aligned} E(\boldsymbol{m}, \boldsymbol{v}) &= E_{exc} + E_{anis} + E_{app} + E_{el} + E_{demag} \\ &= \int_\Omega \frac{C}{2m_s^2}|\nabla \boldsymbol{m}|^2\, \boldsymbol{dx} + \int_\Omega \varphi(\boldsymbol{m})\, \boldsymbol{dx} - \int_\Omega \boldsymbol{h}_a \cdot \boldsymbol{m}\, \boldsymbol{dx} \\ &+ \int_\Omega \frac{1}{2}(\boldsymbol{E} - \boldsymbol{E}_0(\boldsymbol{m})) \cdot \mathbb{C}[\boldsymbol{E} - \boldsymbol{E}_0(\boldsymbol{m})]\, \boldsymbol{dx}. + \frac{1}{8\pi}\int_{\mathbb{R}^3} |\boldsymbol{h_m}|^2\, \boldsymbol{dx}. \end{aligned} \quad (3.3)$$

3.6 Galfenol: Scale of micromagnetic energies

The various energies described, give a complete framework for micromagnetic modeling of magnetostriction. We now look at the values of these energies in comparison with each other. The energies are compared for typical configurations of a long galfenol wire. The Table 3.1 gives typical values of these energies. The 2nd column of Table 3.1 gives the configurations of magnetization for which these energies are calculated.

The table clearly differentiates Galfenol from Terfenol. As opposed to Terfenol, Galfenol is quite soft in terms of anisotropy. The major contribution to energy obviously comes from magnetostatic energy. The value for elastic energy computed is computed as $E_{el} = \frac{1}{2}c_{11}{\lambda_{100}}^2$.

Table 3.1: Energy penalty for various typical configurations

Energy Contribution	penalty for	Energy (ergs/cc)
Exchange energy	domain walls of 60nm	3×10^4
Elastic energy	strains of the order of magnetostrictive strain	6×10^4
Anisotropy energy	magnetization along non-easy axis	3×10^5
Magnetostatic energy	magnetization perpendicular to wire axis	1.3×10^7

Chapter 4

Macroscale modeling for Galfenol beams

In this section we investigate the natural frequencies of a galfenol beam in vibration. The beam diameter is of nanometer size. Later in the section we use the "large-body limit" of the micromagnetic problem as investigated by Antonio Desimone in [DS93]. We conduct calculations based on this model for a millimeter size galfenol beam. This theory can be used to predict "virgin magnetization" curves for ferromagnetic bodies. By virgin magnetization curve we mean the magnetization curve M vs H starting from an ideal demagnetized state when an external field is applied. These predicted curves are then compared with experimental results available for galfenol beams.

The Fig. 4.1 taken from Downey et.al. [DFMS08] shows a galfenol nanowire on an AFM tip vibrating at resonant frequency.

4.1 Natural frequency calculation

Let a beam occupy the region $(0, L) \times S^2_\delta \in \mathbb{R}^3$. Here $x \in (0, L)$ is the space variable which represents the coordinate along the axis of the beam. t is time. ζ is the z-axis deflection where z axis is perpendicular to beam axis. A is the cross-sectional area. ρ is the density. E is the elastic modulus and I is the second moment of area about the neutral axis $(0, L) \times \{0\} \times \{0\}$. We now look at the natural frequency of beams with diameter of nanometer range. The Fig 4.1 shows a nanowire vibrating on an AFM tip.

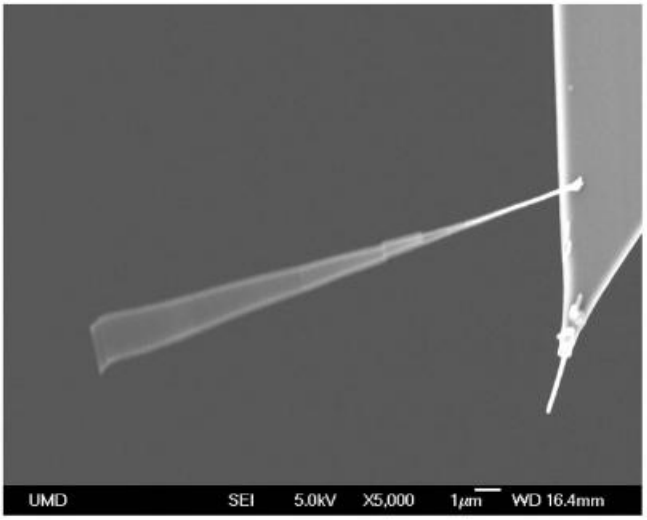

Figure 4.1: Nanowire vibrating on AFM tip

We use the Euler-Bernoulli beam theory and include the rotational inertia term. The book by Karl Graff [Gra91] is a good reference for derivation of vibration models for beam vibration. For our beam we have,

$$EI\frac{\partial^4\zeta(x,t)}{\partial x^4} + A\rho_0\frac{\partial^2\zeta(x,t)}{\partial t^2} - \rho_0 I\frac{\partial^4\zeta(x,t)}{\partial x^2\partial t^2} = 0\ . \tag{4.1}$$

We assume the solution $\zeta(x,t)$ is of the form $\zeta(x,t) = Z(x)T(t)$. Substituting into the governing equation eqn. 4.1 and using separation variable we get,

$$\frac{EIZ''''}{\rho_0 IZ'' - A\rho_0 Z} = \frac{\ddot{T}}{T} = -\omega^2, \quad \text{where } \omega \text{ is the separation constant .}$$

Here "$'$" and "$\cdot$" represent derivative with respect to x and t respectively. Solution for $T(t)$ is given by $T(t) = A\cos\omega t + B\sin\omega t$ with A and B arbitrary constants. The equation for $Z(x)$ is given by,

$$EIZ'''' + \rho_0 I\omega^2 Z'' - A\rho_0\omega^2 Z = 0\ . \tag{4.2}$$

Substituting $Z(x) = e^{\lambda x}$ in 4.2 we get a quartic equation for λ,

$$EI\lambda^4 + \rho_0 I\omega^2\lambda^2 - A\rho_0\omega^2 = 0\ .$$

Solving for λ we get,

$$\lambda^2 = \frac{1}{2}\Big[- \frac{\rho_0 I\omega^2}{EI} \pm \sqrt{\{\frac{\rho_0 I\omega^2}{EI}\}^2 + 4\frac{A\rho_0\omega^2}{EI}}\Big] \ .$$

Since the discriminant of 4.2 $D = \sqrt{(\frac{\rho_0 I\omega^2}{EI})^2 + 4\frac{A\rho_0\omega^2}{EI}} \geq -\frac{\rho_0 I\omega^2}{EI}$, the equation has 2 real and 2 purely imaginary solutions for λ. Let us define α and β,

$$\alpha = \sqrt{\frac{1}{2}\Big[\sqrt{\{\frac{\rho_0 I\omega^2}{EI}\}^2 + 4\frac{A\rho_0\omega^2}{EI}} - \frac{\rho_0 I\omega^2}{EI}\Big]} \quad , \quad \beta = \sqrt{\frac{1}{2}\Big[\sqrt{\{\frac{\rho_0 I\omega^2}{EI}\}^2 + 4\frac{A\rho_0\omega^2}{EI}} + \frac{\rho_0 I\omega^2}{EI}\Big]} \ . \tag{4.3}$$

The four solutions for λ are given by $\lambda_1 = +\alpha, \lambda_2 = -\alpha, \lambda_3 = i\beta, \lambda_4 = -i\beta$. So $Z(x) = C_1 \cosh\alpha x + C_2 \sinh\alpha x + C_3 \cos\beta x + C_4 \sin\beta x$. The boundary conditions for a cantilever beam free at one end and rigidly clamped at the other is,

$$\begin{aligned} Z(x) \mid_{x=0} = Z(0) = 0, \qquad & Z'(x) \mid_{x=0} = Z'(0) = 0, \\ Z''(x) \mid_{x=L} = Z''(L) = 0, \qquad & Z'''(x) \mid_{x=L} = Z'''(L) = 0 \ . \end{aligned}$$

Substituting the form for $Z(x)$ in the boundary conditions at $x = 0$, we get $C_3 = -C_1, C_4 = -\frac{\alpha}{\beta}C_2$. Using the boundary conditions at the free boundary $x = L$ we get,

$$Z''(L) = \{\alpha^2 \cosh\alpha L + \beta^2 \cos\beta L\}C_1 + \{\alpha^2 \sinh\alpha L + \alpha\beta \sin\beta L\}C_2 = 0 \ , \tag{4.4}$$

$$Z'''(L) = \{\alpha^3 \sinh\alpha L - \beta^3 \sin\beta L\}C_1 + \{\alpha^3 \cosh\alpha L + \alpha\beta^2 \cos\beta L\}C_2 = 0 \ . \tag{4.5}$$

To have a non-trivial solution for C_1, C_2 from equations 4.4 and 4.5 we need,

$$\begin{aligned} &\{\alpha^2 \cosh\alpha L + \beta^2 \cos\beta L\}\{\alpha^3 \cosh\alpha L + \alpha\beta^2 \cos\beta L\} - \{\alpha^3 \sinh\alpha L \\ &-\beta^3 \sin\beta L\}\{\alpha^2 \sinh\alpha L + \alpha\beta \sin\beta L\} = 0 \ . \end{aligned} \tag{4.6}$$

On multiplying out we get,

$$\big(\alpha^4 + \beta^4\big) + 2\alpha^2\beta^2 \cosh\alpha L \cos\beta L + \big(\alpha\beta^3 - \alpha^3\beta\big) \sinh\alpha L \sin\beta L = 0 \ .$$

Using the expression 4.3 for α, β in terms of ω the above equation can be written only in terms of ω. The solution are presented in Table 4.1 which gives the values of the natural frequencies for the first few modes.

Table 4.1: First few mode frequencies in Hz. for wires of different lengths

Mode No.	20	40	60	80	100
1	52978	13245	5887	3311	2119
2	332006	83002	36890	20751	13281
3	929618	232407	102392	58102	37185
4	1821654	455423	202411	113857	72868
5	3011263	752843	334599	188213	120456
6	4498188	1124610	499832	281157	179941
7	6282395	1570724	698110	392689	251322

4.2 Virgin magnetization curves for macroscale beams

In this section we return to the variational framework which we called as Brown's model. We use the work of Antonia Desimone [DS93], which deals with the prediction of virgin magnetization curves under the simplifying assumption of large body limit for a ferromagnetic body. This assumption helps us to throw away the exchange energy term from the energy. This can be intuitively seen if we notice the scaling of different energy terms in Brown's model with respect to volume. The argument has been made rigorous by using the mathematical tool of Γ-convergence. As in Desimone's work, for only this section we use only the ferromagnetic energies and completely neglect the elastic energy.

For simplicity we assume the body $\bar{\Omega}$ is a cube with a typical length scale of L and a volume L^3. Let $\bar{\boldsymbol{m}}(\bar{\boldsymbol{x}})$ be the magnetization, $\bar{\boldsymbol{h}}_{\bar{\boldsymbol{m}}}(\bar{\boldsymbol{x}})$ be the demagnetization field and $\bar{\boldsymbol{h}}_a(\bar{\boldsymbol{x}})$ be the applied field. We resize the body by L i.e. map $\bar{\boldsymbol{x}} \mapsto \boldsymbol{x} = \frac{\bar{\boldsymbol{x}}}{L}$, so that $\bar{\Omega} \mapsto \Omega$. The magnetization vector is mapped to new body Ω as follows $\boldsymbol{m}(\boldsymbol{x}) = \bar{\boldsymbol{m}}(\bar{\boldsymbol{x}}$. The demag field is rescaled as $\boldsymbol{h}_{\boldsymbol{m}}(\boldsymbol{x}) = \bar{\boldsymbol{h}}_{\bar{\boldsymbol{m}}}(\bar{\boldsymbol{x}})$. Applied field is rescaled as $\boldsymbol{h}_a(\boldsymbol{x}) = \bar{\boldsymbol{h}}_a(\bar{\boldsymbol{x}})$. Noting that the Jacobian of the transformation $\bar{\Omega} \mapsto \Omega$ is L^3, the energy per unit volume becomes,

$$\begin{aligned}
\frac{1}{L^3}E(\bar{\boldsymbol{m}}) &= \frac{1}{L^3}\int_{\bar{\Omega}} \Big(C|\nabla\bar{\boldsymbol{m}}|^2 + \varphi(\bar{\boldsymbol{m}}) - \bar{\boldsymbol{h}}_a \cdot \bar{\boldsymbol{m}}\Big)\, d\bar{\boldsymbol{x}} + \frac{1}{L^3}\int_{\mathbb{R}^3} |\bar{\boldsymbol{h}}_{\bar{\boldsymbol{m}}}|^2\, d\bar{\boldsymbol{x}}, \\
&= \frac{1}{L^3}\int_{\Omega} \Big(C\frac{1}{L^2}|\nabla\boldsymbol{m}|^2 + \varphi(\boldsymbol{m}) - \boldsymbol{h}_a \cdot \boldsymbol{m}\Big)L^3\, d\boldsymbol{x} + \frac{1}{L^3}\int_{\mathbb{R}^3} |\boldsymbol{h}_{\boldsymbol{m}}(\boldsymbol{x})|^2 L^3\, d\boldsymbol{x}, \\
&= \int_{\Omega} \Big(C\frac{1}{L^2}|\nabla\boldsymbol{m}|^2 + \varphi(\boldsymbol{m}) - \boldsymbol{h}_a \cdot \boldsymbol{m}\Big)\, d\boldsymbol{x} + \int_{\mathbb{R}^3} |\boldsymbol{h}_{\boldsymbol{m}}(\boldsymbol{x})|^2\, d\boldsymbol{x}, \\
&= E_L(\boldsymbol{m})\ . \qquad (4.7)
\end{aligned}$$

The micromagnetic problem as defined by Brown [Bro63] thus becomes,

$$(\mathcal{P}_L) \quad \inf_{\boldsymbol{m}\in H^1(\Omega, m_s S^2)} E_L(\boldsymbol{m}). \qquad (4.8)$$

The $(\mathcal{P}_L)$ are a sequence of problems, and the Γ-limit analysis is to define a new problem

$$(\mathcal{P}_\infty) \qquad \inf_{\boldsymbol{m}\in\mathcal{A}} E_\infty(\boldsymbol{m}) \qquad \mathcal{A} \text{ is appropriate function space .} \qquad (4.9)$$

such that the energy $E_\infty(\boldsymbol{m})$ is a Γ-limit of the energies $E_L(\boldsymbol{m})$. The definition of Γ-convergence and its properties is given in Braides [Bra02]. In formal terms it is the

convergence of the variational problem $E_L(\boldsymbol{m})$ in some appropriate sense to $E_\infty(\boldsymbol{m})$ and the minimizer $\boldsymbol{m}_L$ of $(\mathcal{P}_L)$ converges to the minimizer $\boldsymbol{m}_\infty$ of $(\mathcal{P}_\infty)$ as the parameter $L \to \infty$. As per DeSimone [DS93] the Γ-limit problem $(\mathcal{P}_\infty)$ is given by,

$$(\mathcal{P}_\infty) \quad \inf_{\boldsymbol{m}\in L^2(\Omega,\mathbb{R}^3):|\boldsymbol{m}|\le m_s} E_\infty(\boldsymbol{m}) = \int_\Omega \varphi^{**}(\boldsymbol{m})\, \boldsymbol{dx} - \int_\Omega \boldsymbol{h}_a \cdot \boldsymbol{m}\, \boldsymbol{dx} - \frac{1}{2}\int_\Omega \boldsymbol{h}_m \cdot \boldsymbol{m}\, \boldsymbol{dx}\ . \quad (4.10)$$

$\varphi^{**}(\boldsymbol{m})$ in the above equation is the convexification of $\varphi(\boldsymbol{m})$ which is defined as the highest convex function majorized by φ,

$$\varphi^{**}(\boldsymbol{m}) = \sup\{f(\boldsymbol{m}) : f \in \text{ convex, and } f \le \varphi\}\ .$$

An alternate characterization is given by Dacarogna [Dac89],

$$\varphi^{**}(\boldsymbol{m}) = \inf\Big\{ \sum_{k=1}^{4} \lambda_k \varphi(\boldsymbol{m}_k) : \sum_{k=1}^{4} \lambda_k \boldsymbol{m}_k = \boldsymbol{m} \ \ \& \ \ \sum_{k=1}^{4} \lambda_k = 1, \boldsymbol{m}_k \in m_s S^2 \Big\}\ . \quad (4.11)$$

Note that in the problem $\mathcal{P}_\mathcal{L}$, as the size of the body increases, the contribution of the exchange energy to the overall energy gets monotonically smaller. The limiting theory thus can be expected to have negligible exchange energy. However note that exchange is a convex energy term of the highest order. As its contribution gets smaller minimizing sequences of $\mathcal{P}_\mathcal{L}$ to develop finer and finer scale oscillations of magnetization. Thus the Γ-limit problem no longer has the exchange term and its set of admissible functions has to be expanded to include the limit of the fine scale oscillations. Mathematically speaking, neglecting the exchange energy causes minimizing sequences for the energy to loose compactness so that the sequences don't converge strongly. The set of admissible functions needs to be expanded to include the weak limits of the minimizing sequences. This is the reason, the constraint $|\boldsymbol{m}| = m_s$ in $\mathcal{P}_\mathcal{L}$ is weakened to $|\boldsymbol{m}| \le m_s$ in $\mathcal{P}_\infty$ and the limit problem models the weak limit of sequences which physically represent the average magnetization in the body.

The form of the Magnetocrystalline energy is as follows,

$$\varphi(\boldsymbol{m}) = \frac{K_1}{{m_s}^4}\{{m_x}^2{m_y}^2 + {m_y}^2{m_z}^2 + {m_x}^2{m_z}^2\} + \frac{K_2}{{m_s}^6}\{{m_x}^2{m_y}^2{m_z}^2\} \qquad \forall \boldsymbol{m} \in m_s S^2\ .$$

Define $\tilde{\Omega} := \{\boldsymbol{x} : \boldsymbol{x} \in \Omega \quad \& \quad |\boldsymbol{m}(\boldsymbol{x})| < m_s\}$. Minimization of $\mathcal{P}_\infty$ leads to the following variational inequality,

$$D\varphi^{**}(\boldsymbol{m}) - (\boldsymbol{h}_a + \boldsymbol{h}_{\boldsymbol{m}}) = 0 \qquad \forall \boldsymbol{x} \in \tilde{\Omega}\ , \quad (4.12)$$

$$D\varphi^{**}(\boldsymbol{m}) - (\boldsymbol{h}_a + \boldsymbol{h}_m) = \gamma \boldsymbol{m} \qquad \gamma \le 0, \quad \forall \boldsymbol{x} \in \Omega \setminus \tilde{\Omega}\ . \quad (4.13)$$

We set now, $\boldsymbol{h}_a = \tau \boldsymbol{u}$, where $\boldsymbol{u}$ is the unit vector in the direction of the applied field $\boldsymbol{h}_a$ and τ is the scalar magnitude of the field.

$$D\varphi^{**}(\boldsymbol{m}) - (\tau \boldsymbol{u} + \boldsymbol{h}_m) = 0 \qquad \forall \boldsymbol{x} \in \tilde{\Omega} \ , \tag{4.14}$$

$$D\varphi^{**}(\boldsymbol{m}) - (\tau \boldsymbol{u} + \boldsymbol{h}_m) = \gamma \boldsymbol{m} \qquad \gamma \leq 0, \quad \forall \boldsymbol{x} \in \Omega \setminus \tilde{\Omega} \ . \tag{4.15}$$

The $\varphi^{**}(\boldsymbol{m})$ is hard to calculate analytically for the cubic anisotropy function as above. As remarked by Desimone however, we can calculate the form of $\varphi^{**}(\boldsymbol{m})$ along some crystallographic families of high symmetry like $\langle 100 \rangle, \langle 110 \rangle, \langle 111 \rangle$ etc. We use this fact to predict virgin magnetization curves for millimeter size galfenol cantilevers which we model as long thin cylinders.

Till the end of this section we assume the wire is aligned with its axis along the z-coordinate axis. For such wires, with large aspect ratio, $\boldsymbol{h_m}$ and is give through a linear function of $\boldsymbol{m}$ through operation by the demagnetization tensor $\boldsymbol{D}$.

$$\boldsymbol{h_m} = -\boldsymbol{D}\boldsymbol{m} \qquad \text{where} \qquad \boldsymbol{D} \approx 4\pi \begin{bmatrix} \frac{1}{2} & 0 & 0 \\ 0 & \frac{1}{2} & 0 \\ 0 & 0 & 0 \end{bmatrix}$$

We also specify that in the course of this investigation the term "large body model" will always refer to the problem $\mathcal{P}_\infty$ as defined in 4.10

4.2.1 Wire axis along $\langle 100 \rangle$ direction

In this subsection z-coordinate axis is the $\langle 100 \rangle$ crystallographic axis. Fig.(4.2) shows the orientation of wire and crystallographic axis w.r.t. coordinate axes. Let $\boldsymbol{e}_i$ be the unit vectors along coordinate axis, with $i = x, y, z$.

A. Magnetization parallel to wire axis

For magnetizations along the $\langle 100 \rangle$ direction family,if $\boldsymbol{m} = \nu m_s \boldsymbol{u}$ where $\boldsymbol{u} = \boldsymbol{e}_z$ is unit vector along $\langle 100 \rangle$ direction and $\nu \leq 1$, we can choose $\boldsymbol{m}_k$ in eqn.(4.11) as $\boldsymbol{m}_1 = m_s \boldsymbol{e}_z$, $\boldsymbol{m}_2 = -m_s \boldsymbol{e}_z$. Also set $\lambda_1 = \frac{1+\nu}{2}$ and $\lambda_2 = \frac{1-\nu}{2}$. From [DS93] we have,

$$\varphi^{**}(\boldsymbol{m}) = \lambda_1 \varphi(\boldsymbol{m}_1) + \lambda_2 \varphi(\boldsymbol{m}_2) \equiv 0, \quad \forall \boldsymbol{m} = \nu m_s \boldsymbol{u} \ .$$

$$D\varphi^{**}(\boldsymbol{m}) = 0 \qquad \forall \boldsymbol{m} = \nu m_s \boldsymbol{u} \ .$$

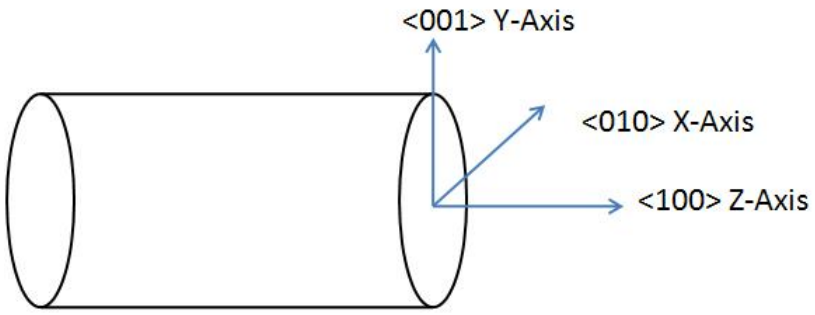

Figure 4.2: Orientation of wire w.r.t. coordinate and crystallographic axis

Case 1 : $|\boldsymbol{m}(x)| < m_s \quad \forall \boldsymbol{x} \in \Omega.$

Equation(4.14) gives us,

$$\tau \boldsymbol{u} + \boldsymbol{h_m} = D\varphi^{**}(\boldsymbol{m}) = 0 \ .$$

Thus $\tau \boldsymbol{u} = -\boldsymbol{h_m} = \boldsymbol{D}\boldsymbol{m}$.

Taking vector dot product of both sides with $\boldsymbol{u}$

$$\tau = \boldsymbol{u} \cdot \boldsymbol{D}\boldsymbol{m} = \boldsymbol{m} \cdot \boldsymbol{D}^T \boldsymbol{u} = m_z D_{zz} = 0 \qquad \text{as } \boldsymbol{u} \text{ is z-axis direction.}$$

Thus, $\tau = 0$, when $|\boldsymbol{m}(x)| < m_s$.

Case 2 : $|\boldsymbol{m}(x)| = m_s \quad \forall \boldsymbol{x} \in \Omega.$

Eqn(4.15) gives us,

$$\tau \boldsymbol{u} + \boldsymbol{h}_m = D\varphi^{**}(\boldsymbol{m}) - \gamma \boldsymbol{m} = -\gamma \boldsymbol{m} \ .$$

Taking vector dot product of both sides with $\boldsymbol{u}$

$$\tau = D_{zz} m_z - \gamma m_s = -\gamma m_s \ .$$

B. Magnetization perpendicular to wire axis

Here the field is applied perpendicular to axis, along the $\langle 001 \rangle$ directions shown as the y axis in Fig.(4.2) which induces magnetization $\boldsymbol{m}$ along $\langle 001 \rangle$. Set $\boldsymbol{u} = \boldsymbol{e}_y$ as unit vector along $\langle 001 \rangle$. So $\boldsymbol{m} = \nu m_s \boldsymbol{u}, \quad \nu \leq 1$. We can check that for $\boldsymbol{m}$ along $\langle 001 \rangle$ $\varphi^{**}(\boldsymbol{m}) \equiv 0$ and $D\varphi^{**}(\boldsymbol{m}) \equiv 0$ from the reference [DS93].

Case 1 : $|\boldsymbol{m}(x)| < m_s \quad \forall \boldsymbol{x} \in \Omega$.

Equation(4.14) gives us,

$$\tau \boldsymbol{u} + \boldsymbol{h_m} = D\varphi^{**}(\boldsymbol{m}) = 0 \ .$$
$$\text{Thus } \tau \boldsymbol{u} = -\boldsymbol{h_m} = \boldsymbol{D}\boldsymbol{m} \ .$$

Taking vector dot product of both sides with $\boldsymbol{u}$

$$\tau = \boldsymbol{u} \cdot \boldsymbol{D}\boldsymbol{m} = \boldsymbol{m} \cdot \boldsymbol{D}^T \boldsymbol{u} = m_y D_{yy}, \qquad \boldsymbol{u} \text{ is y-axis direction.}$$
$$= \frac{4\pi \langle \boldsymbol{m}, \boldsymbol{u} \rangle}{2} = 2\pi \langle \boldsymbol{m}, \boldsymbol{u} \rangle \ .$$

Case 2 : $|\boldsymbol{m}(x)| = m_s \quad \forall \boldsymbol{x} \in \Omega$.

Eqn(4.15) gives us,

$$\tau \boldsymbol{u} + \boldsymbol{h_m} = D\varphi^{**}(\boldsymbol{m}) - \gamma \boldsymbol{m} = -\gamma \boldsymbol{m} \ .$$

Taking vector dot product of both sides with $\boldsymbol{u}$

$$\tau = m_y D_{yy} - \gamma m_y, \qquad \boldsymbol{u} \text{ is y-axis direction.}$$
$$= (\frac{4\pi}{2} - \gamma) \langle \boldsymbol{m}, \boldsymbol{u} \rangle = (2\pi - \gamma) m_s \ .$$

Figure 4.3 is a plot of the results of Case A and Case B for wires oriented along $\langle 100 \rangle$ axis. The Y-axis is the magnetization in emu/cc, with the X-axis showing applied field in oerstads.

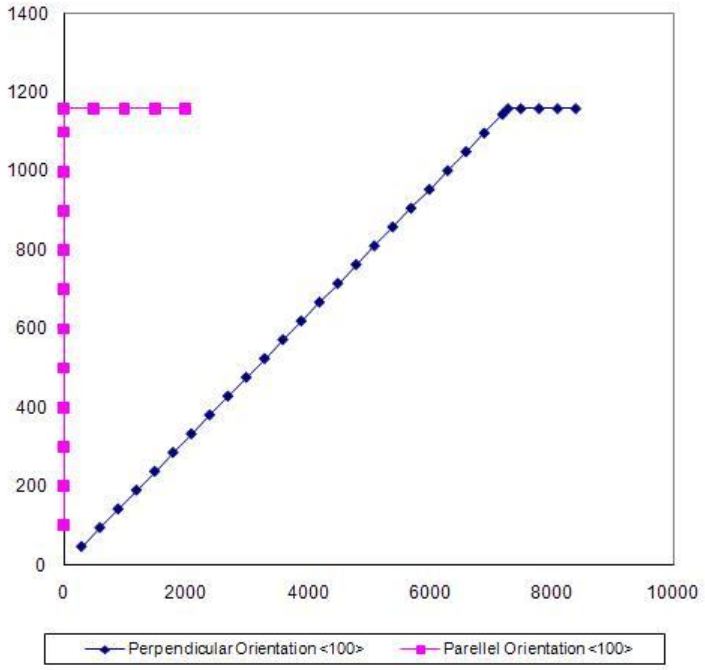

Figure 4.3: Virgin curves perpendicular and parallel to 100 direction wire axis

4.2.2 Wire axis along $\langle 110 \rangle$ direction

Fig.(4.4) shows orientations of crystallographic and wire axis w.r.t. coordinate axis.

For this section we need values for some physical constants. We use the values for these constants for galfenol alloy with 8.5 % Ga. $K_1 = 70kJ/(m^3) = 700kerg/cc$, $m_s = 1.9T \approx 1600emu$.

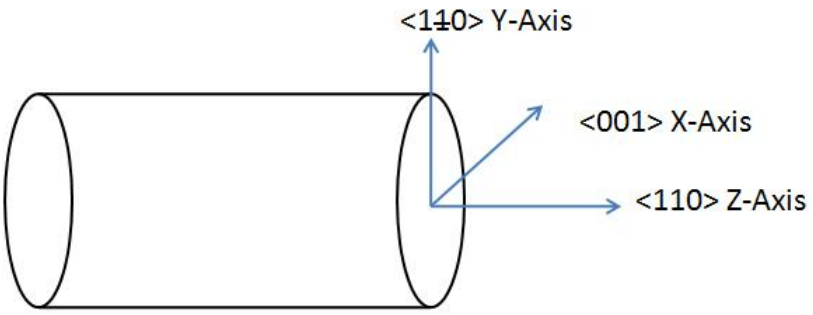

Figure 4.4: Orientation of wire w.r.t. coordinate and crystallographic axis

A. Magnetization parallel to wire axis

From [DS93] we have,

$$\varphi^{**}(\boldsymbol{m}) = \begin{cases} 0 & \forall \quad |\boldsymbol{m}(\boldsymbol{x})| \leq \frac{m_s}{\sqrt{2}} \\ \frac{K_1}{m_s^4}(|\boldsymbol{m}|^2 - \frac{m_s^2}{2})^2 & \forall \quad \frac{m_s}{\sqrt{2}} \leq |\boldsymbol{m}(\boldsymbol{x})| \leq m_s \ . \end{cases}$$

$$D\varphi^{**}(\boldsymbol{m}) = \begin{cases} 0 & \forall \quad |\boldsymbol{m}(\boldsymbol{x})| \leq \frac{m_s}{\sqrt{2}} \\ \frac{4K_1}{m_s^4}\boldsymbol{m}(|\boldsymbol{m}|^2 - \frac{m_s^2}{2}) & \forall \quad \frac{m_s}{\sqrt{2}} \leq |\boldsymbol{m}(\boldsymbol{x})| \leq m_s \ . \end{cases}$$

Case 1 : $|\boldsymbol{m}(\boldsymbol{x})| \leq \frac{m_s}{\sqrt{2}} \quad \forall \boldsymbol{x} \in \Omega.$

Eqn.(4.14) gives us,

$$\tau \boldsymbol{u} + \boldsymbol{h_m} = D\varphi^{**}(\boldsymbol{m}) = 0 \ . \tag{4.16}$$

Taking vector dot product of both sides with $\boldsymbol{u}$,

$$\tau = m_z D_{zz} = 0, \quad \boldsymbol{u} \text{ is z-axis direction} \ . \tag{4.17}$$

Thus $\tau = 0$ till $|\boldsymbol{m}(\boldsymbol{x})| \leq \dfrac{m_s}{\sqrt{2}} = \dfrac{1600}{\sqrt{2}} emu \approx 1130 emu$.

Case 2 : $\frac{m_s}{\sqrt{2}} \leq |\boldsymbol{m}(\boldsymbol{x})| < m_s \quad \forall \boldsymbol{x} \in \Omega.$

Eqn.(4.14) give us,

$$\tau \boldsymbol{u} + \boldsymbol{h_m} = D\varphi^{**}(\boldsymbol{m}) = \frac{4K_1}{m_s^4}\boldsymbol{m}(|\boldsymbol{m}|^2 - \frac{m_s^2}{2}) \ . \tag{4.18}$$

Taking vector dot product of both sides with $\boldsymbol{u}$,

$$\tau = m_z D_{zz} + \frac{4K_1}{m_s^4}(|\boldsymbol{m}|^2 - \frac{m_s^2}{2})\langle \boldsymbol{m}, \boldsymbol{u}\rangle = \frac{4K_1}{m_s^4}(|\boldsymbol{m}|^2 - \frac{m_s^2}{2})\langle \boldsymbol{m}, \boldsymbol{u}\rangle \ . \tag{4.19}$$

As $|\boldsymbol{m}| \ \rightarrow m_s = 1600emu$,

$$\tau \rightarrow \tau_{cr} = \frac{4K_1}{m_s^4} m_s({m_s}^2 - \frac{m_s^2}{2}) = \frac{2K_1}{m_s} = 0.875KOe \ .$$

Case 3 : $|\boldsymbol{m}(\boldsymbol{x})| = m_s \quad \forall \boldsymbol{x} \in \Omega$.

Eqn.(4.15) gives us,

$$\tau \boldsymbol{u} + \boldsymbol{h}_m = D\varphi^{**}(m_s) - \gamma \boldsymbol{m} = \frac{2K_1}{m_s^2}\boldsymbol{m} - \gamma \boldsymbol{m} \ . \tag{4.20}$$

Taking vector dot product of both sides with $\boldsymbol{u}$,

$$\tau = m_z D_{zz} + \frac{2K_1}{m_s} - \gamma\langle \boldsymbol{m}, \boldsymbol{u}\rangle = 0.875KOe - \gamma \boldsymbol{m}_s, \qquad \boldsymbol{u} \text{ is z-axis direction.} \tag{4.21}$$

B. Magnetization perpendicular to wire axis

We assume the perpendicular direction (y-axis) is also a $\langle 110\rangle$ direction. From [DS93] we have,

$$\varphi^{**}(\boldsymbol{m}) = \begin{cases} 0 & \forall \quad |\boldsymbol{m}(\boldsymbol{x})| \leq \frac{m_s}{\sqrt{2}} \\ \frac{K_1}{m_s^4}(|\boldsymbol{m}|^2 - \frac{m_s^2}{2})^2 & \forall \quad \frac{m_s}{\sqrt{2}} \leq |\boldsymbol{m}(\boldsymbol{x})| \leq m_s \ . \end{cases}$$

$$D\varphi^{**}(\boldsymbol{m}) = \begin{cases} 0 & \forall \quad |\boldsymbol{m}(\boldsymbol{x})| \leq \frac{m_s}{\sqrt{2}} \\ \frac{4K_1}{m_s^4}\boldsymbol{m}(|\boldsymbol{m}|^2 - \frac{m_s^2}{2}) & \forall \quad \frac{m_s}{\sqrt{2}} \leq |\boldsymbol{m}(\boldsymbol{x})| \leq m_s \ . \end{cases}$$

Case 1 : $|\boldsymbol{m}(\boldsymbol{x})| \leq \frac{m_s}{\sqrt{2}} \quad \forall \boldsymbol{x} \in \Omega$.

Eqn.(4.14) becomes,

$$\tau \boldsymbol{u} + \boldsymbol{h_m} = D\varphi^{**}(\boldsymbol{m}) = 0 \ . \tag{4.22}$$

Taking vector dot product of both sides with $\boldsymbol{u}$,

$$\tau = m_y D_{yy} = 2\pi \langle \boldsymbol{m}, \boldsymbol{u} \rangle, \qquad \boldsymbol{u} \text{ is y-axis direction.} \tag{4.23}$$

When $|\boldsymbol{m}| = \dfrac{m_s}{\sqrt{2}} = 1130emu$ then $\tau = 2\pi * 1.130kemu \approx 7.1KOe$.

Case 2 : $\frac{m_s}{\sqrt{2}} \leq |\boldsymbol{m}(\boldsymbol{x})| < m_s \quad \forall \boldsymbol{x} \in \Omega.$

Eqn.(4.14) give us,

$$\tau \boldsymbol{u} + \boldsymbol{h_m} = D\varphi^{**}(\boldsymbol{m}) = \frac{4K_1}{m_s^4} \boldsymbol{m} (|\boldsymbol{m}|^2 - \frac{m_s^2}{2}) \ . \tag{4.24}$$

Taking vector dot product of both sides with $\boldsymbol{u}$,

$$\begin{aligned} \tau &= m_y D_{yy} + \frac{4K_1}{m_s^4}(|\boldsymbol{m}|^2 - \frac{m_s^2}{2}) \langle \boldsymbol{m}, \boldsymbol{u} \rangle = \{2\pi + \frac{4K_1}{m_s^4}(|\boldsymbol{m}|^2 - \frac{m_s^2}{2})\} \langle \boldsymbol{m}, \boldsymbol{u} \rangle, \\ & \boldsymbol{u} \text{ is y-axis direction.} \end{aligned} \tag{4.25}$$

When,$\boldsymbol{m} \to m_s$,

$$\begin{aligned} \tau \to \tau_{cr} &= 2\pi m_s + \frac{4K_1}{m_s^4} m_s (m_s^2 - \frac{m_s^2}{2}) = 2\pi m_s + \frac{2K_1}{m_s}, \\ &= 2\pi * 1.6KOe + 0.875KOe \approx 10.9KOe \ . \end{aligned} \tag{4.26}$$

Case 3 : $|\boldsymbol{m}(\boldsymbol{x})| = m_s \quad \forall \boldsymbol{x} \in \Omega.$

Eqn.(4.15) gives us,

$$\tau \boldsymbol{u} + \boldsymbol{h_m} = D\varphi^{**}(\boldsymbol{m}) - \gamma \boldsymbol{m} = \frac{2K_1}{m_s^2} \boldsymbol{m} - \gamma \boldsymbol{m} \ . \tag{4.27}$$

Taking vector dot product of both sides with $\boldsymbol{u}$,

$$\tau = m_y D_{yy} + \frac{2K_1}{m_s} - \gamma \boldsymbol{m} = 10.9KOe - \gamma m_s, \qquad \boldsymbol{u} \text{ is y-axis direction.} \tag{4.28}$$

Fig 4.5 is a plot of the virgin magnetization curves for wires aligned along $\langle 110 \rangle$ crystal axis.

The Fig 4.6 provides a comparison between the virgin magnetization curves predicted and VSM hysteresis curves for galfenol samples.

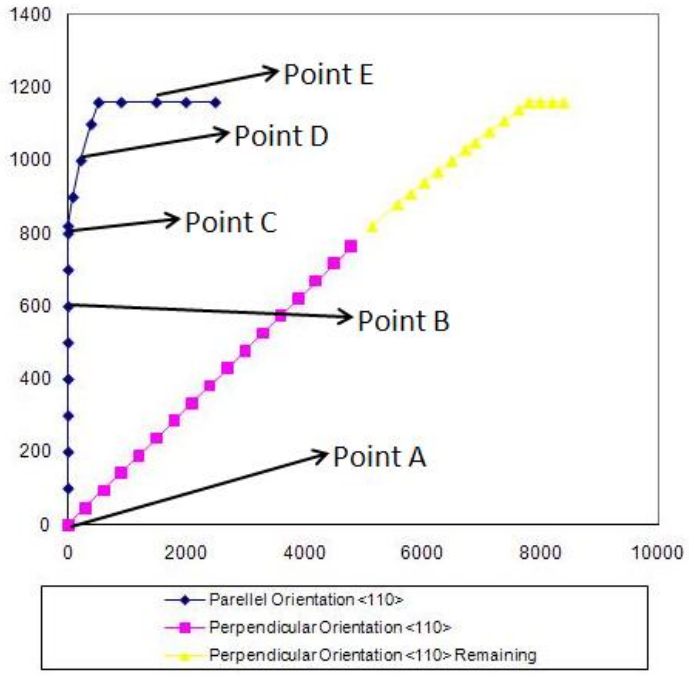

Figure 4.5: Virgin curves perpendicular and parallel to 110 direction wire axis

4.2.3 Domain microstructure along virgin magnetization curve

Not only does the large body limit 4.10 give us the virgin magnetization curves, it also gives us information regarding the domain microstructure through the knowledge of the $\boldsymbol{m}_k$ which solve for $\varphi^{**}(\boldsymbol{m})$ in the equation 4.11. One can show that these $\boldsymbol{m}_k$ along with the λ_k in eqn. 4.11 form the domain orientations and corresponding volume fractions which constitute the microstructre at any point along the virgin magnetization curve. The figures below gives us an illustration of these calculations at various points on the virgin curve for magnetization along the wire axis for $\langle 110 \rangle$ oriented axis. The points have been indexed in the Fig.(4.5) as point A,B,C,D and E.

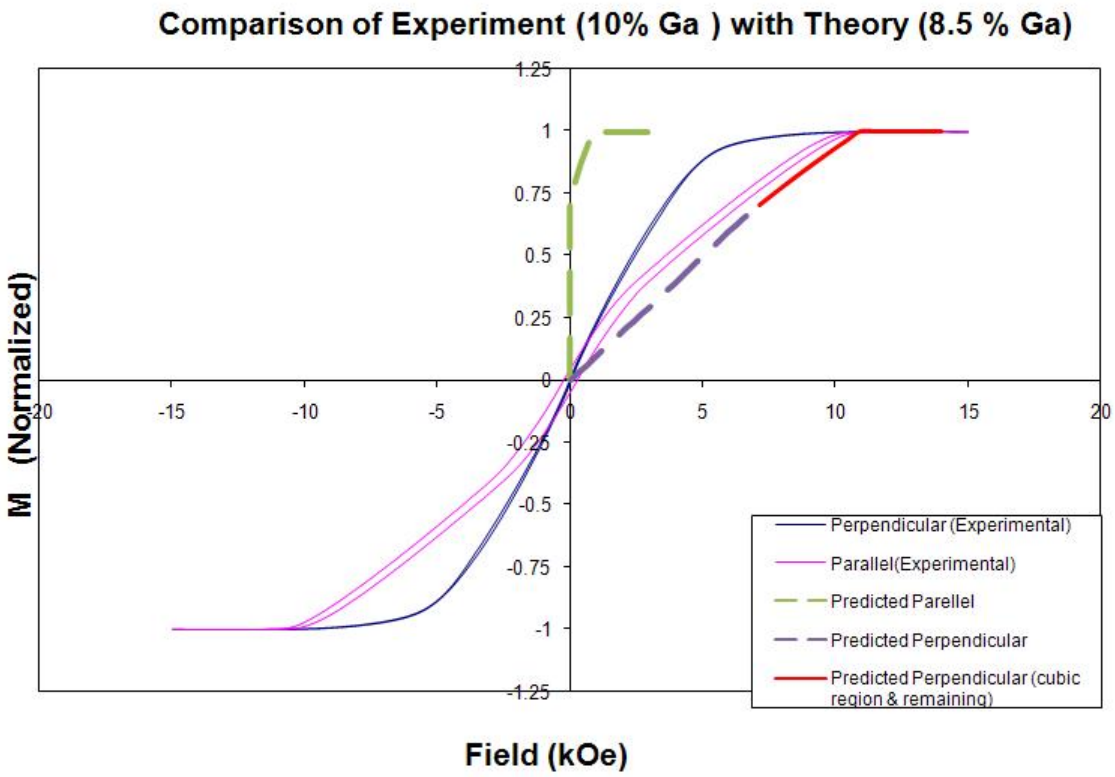

Figure 4.6: Comparison with hysteresis data

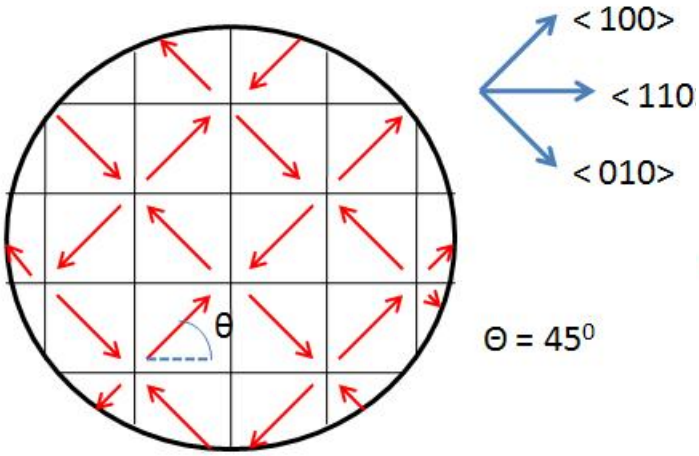

Figure 4.7: Domain microstructure at pointA

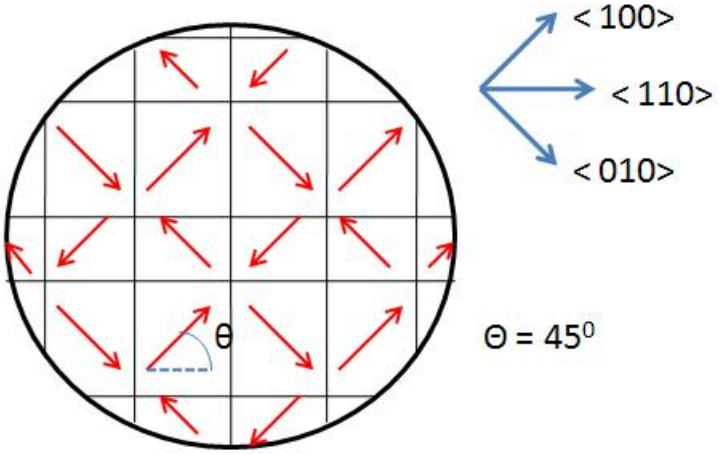

Figure 4.8: Domain microstructure at pointB

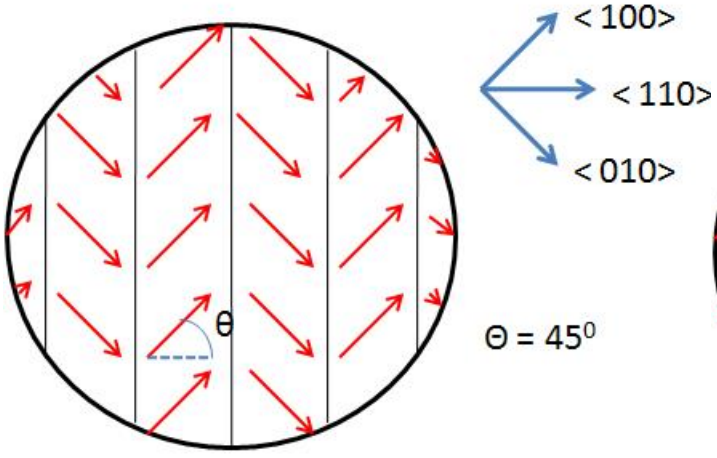

Figure 4.9: Domain microstructure at pointC

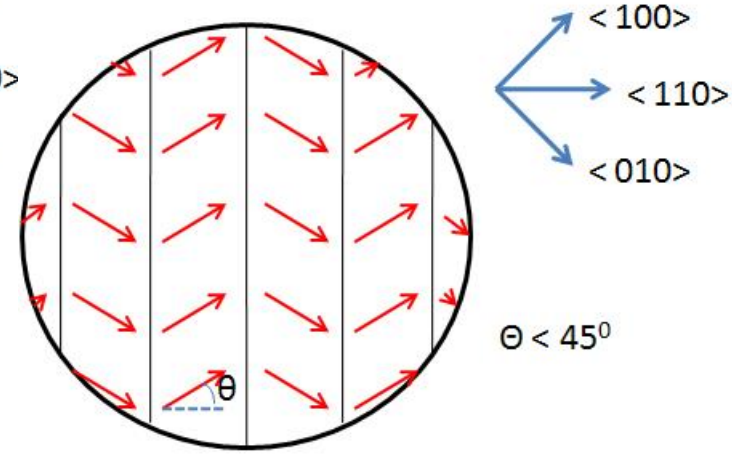

Figure 4.10: Domain microstructure at pointD

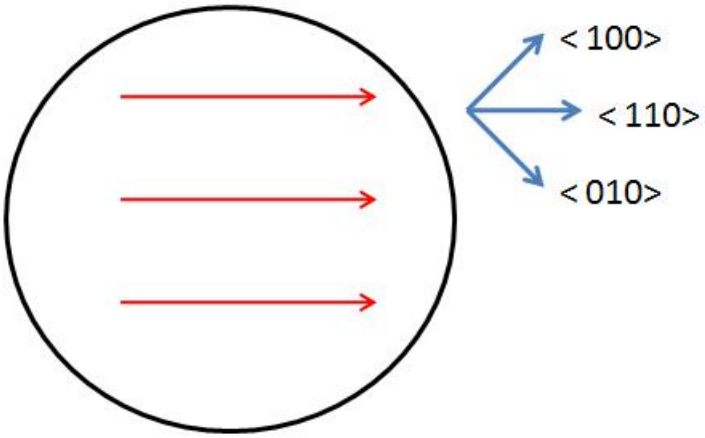

Figure 4.11: Domain microstructure at pointE

4.3 Domain size calculation

The "large body limit" and predicted domain patterns of the previous section can be used to get a sense of the scale of domain sizes. We consider a wire of rectangular cross section for simplicity, of length L, breadth b and width h. We add closure domains to the domain pattern calculated in the previous section to get what is known in the literature as Landau-Lifschitz structure. The governing logic behind the Landau-Lifschitz structure is to construct closure domain pattern so as to completely eliminate the demagnetization energy. If s is the domain width, we then can minimize the total energy, with the respect to domain width. Let Γ be the wall energy. Inspite of the huge difference in the structure of domain walls, the value of Γ lies in the range of 1-2 erg/cm^2 for all kinds of known wall configurations e.g Bloch wall, Nell wall etc. So we take it to be 1 erg/cm^2 for the sake of calculation. K_{11} is the anisotropy constant which is 30 KJ/m^3. We then get for total energy,

$$\begin{aligned} E(s) &= \text{exchange} + \text{interfacial wall energy} + \text{anisotropy} + \text{magnetostatic} \\ &= 0 + \frac{\Gamma L b h}{s} + \frac{b L K_{11}}{4(\sqrt{2}-1)} + 0 \end{aligned}$$

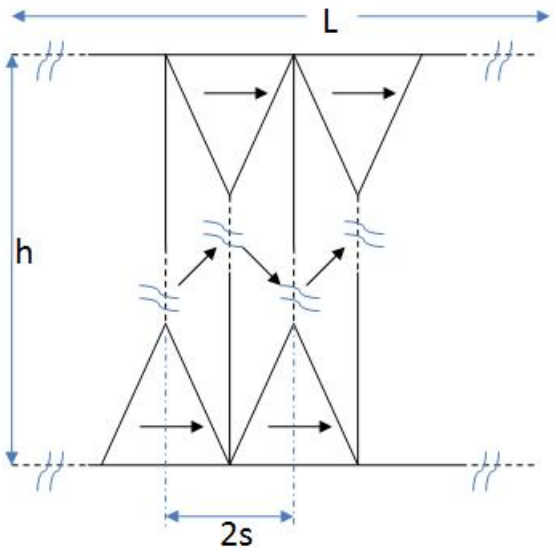

Figure 4.12: Domain shape at point C

Optimizing total energy over the free parameter s we get, $s^2 = \frac{4(\sqrt{2}-1)\Gamma h}{K_{11}}$. Thus $s \approx 8.65\mu m$.

Similar domain width calculations can be done for all of the points on the virgin magnetization curve. Other points will obviously require a different choice of closure domain to eliminate the demagnetization energy. The domain width calculated here is an upper bound to the actual domain width, because we have minimized the energy subject to the constraint of eliminating demagnetization energy. More complicated closure domains can be constructed which may kill of the anisotropy or the exchange energy. Refer to the work of Choksi et.al [CK98] which provide constructions for closure domains which may be energetically more favourable than the Landau-Lifschitz closure domains. The main idea here is to determine regimes of scales depending upon material and geometrical parameters like length of body, exchange constant, anisotropy constant etc. and to provide closure domain constructions which provide "minimum energy" in terms of asymptotic scaling laws with respect to those regimes.

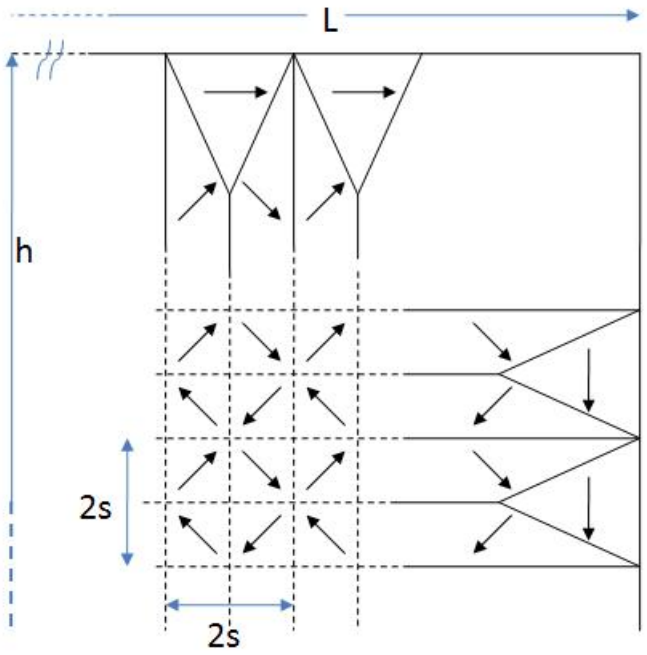

Figure 4.13: Closure domain for Landau-Lifschitz pattern at point A

Chapter 5

Rescaled micromagnetics and further calculations

As in previous section we rescale the body and define the minimization problem for magnetostriction as a new rescaled minimization problem. Let $\hat{\mathbf{x}} \in \hat{\Omega}$ be the body. In this chapter $\hat{\Omega}$ is always identified to be a prolate ellipsoid of major axis L along the $z$coordinate direction and semi-minor axis R along $x-y$ coordinates.Let $\hat{\mathbf{m}}(\hat{\mathbf{x}})$ is the magnetization, the demagnetization field is $\hat{\mathbf{h}}_{\mathbf{m}}(\hat{\mathbf{x}})$, $\hat{\mathbf{h}}_{\mathbf{a}}(\hat{\mathbf{x}})$ is the applied field and $\hat{\mathbf{u}}(\hat{\mathbf{x}})$ be the displacement.

We rescale the body $\hat{\Omega}$ to new body Ω as follows:

$$\mathbf{x} = \frac{\hat{\mathbf{x}}}{R} \tag{5.1}$$

Note that the rescaling makes Ω a prolate ellipsoid with major axis $\frac{L}{2R}$ and semi-minor axis 1. The magnetization vector for the new body $\hat{\Omega}$ is assigned as,

$$\mathbf{m}(\mathbf{x}) = \frac{\hat{\mathbf{m}}(\hat{\mathbf{x}})}{m_s} \qquad \mathbf{h}_{\mathbf{m}}(\mathbf{x}) = \frac{\hat{\mathbf{h}}_{\mathbf{m}}(\hat{\mathbf{x}})}{m_s} \tag{5.2}$$

$$\mathbf{h}_{\mathbf{a}}(\mathbf{x}) = \frac{\hat{\mathbf{h}}_{\mathbf{a}}(\hat{\mathbf{x}})}{m_s} \qquad \mathbf{u}(\mathbf{x}) = \frac{\hat{\mathbf{u}}(\hat{\mathbf{x}})}{R} \tag{5.3}$$

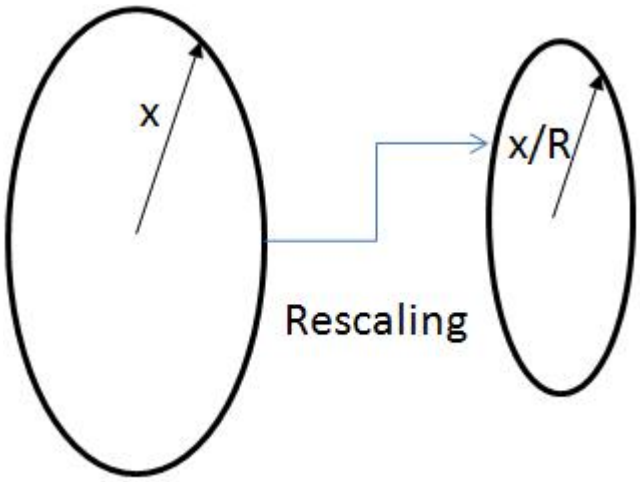

Figure 5.1: Rescaling of domain

From above,

$$\begin{aligned}
\mathbf{E}(\mathbf{x}) &= \frac{\nabla_{\mathbf{x}}\mathbf{u}(\mathbf{x}) + \nabla_{\mathbf{x}}\mathbf{u}(\mathbf{x})^T}{2} \\
&= \frac{1}{R}\cdot\frac{\nabla_{\mathbf{x}}\hat{\mathbf{u}}(\hat{\mathbf{x}}) + \nabla_{\mathbf{x}}\hat{\mathbf{u}}(\hat{\mathbf{x}})^T}{2} \qquad \cdots \text{from eqn.(5.3)} \\
&= \frac{1}{R}\cdot\frac{R\,\nabla_{\hat{\mathbf{x}}}\hat{\mathbf{u}}(\hat{\mathbf{x}}) + R\,\nabla_{\hat{\mathbf{x}}}\hat{\mathbf{u}}(\hat{\mathbf{x}})^T}{2} \qquad \cdots \text{from eqn.(5.1)} \\
&= \frac{\nabla_{\hat{\mathbf{x}}}\hat{\mathbf{u}}(\hat{\mathbf{x}}) + \nabla_{\hat{\mathbf{x}}}\hat{\mathbf{u}}(\hat{\mathbf{x}})^T}{2} = \hat{\mathbf{E}}(\hat{\mathbf{x}})
\end{aligned}$$

The rescaled energy functional per unit volume as a result is,

$$\begin{aligned}
\mathcal{E}(\mathbf{m},\mathbf{u}) &= \int_\Omega \frac{c}{2R^2}|\nabla\mathbf{m}|^2 + \varphi(\mathbf{m}) - m_s^2\mathbf{m}\cdot\mathbf{h}_a + \frac{m_s^2}{8\pi}\int_{\Re^3}|\mathbf{h_m}|^{\mathbf{2}} \\
&\quad + \frac{1}{2}\mathbf{C}\big[\mathbf{E}-\mathbf{E_s}(\mathbf{m})\big] : \big(\mathbf{E}-\mathbf{E_s}(\mathbf{m})\big) \qquad (5.4)
\end{aligned}$$

$$\nabla\cdot(\mathbf{h}_{\bar{m}} + 4\pi\chi_\Omega\mathbf{m}) = 0 \qquad \text{where } |\mathbf{m}| = 1 \qquad (5.5)$$

Since $\mathbf{m}$ has been normalized by m_s to norm $|\mathbf{m}| = 1$,the anisotropy and spontaneous magnetostrictive strain becomes

$$\varphi(\mathbf{m}) = K_1(m_x^2m_y^2 + m_x^2m_z^2 + m_y^2m_z^2) + K_2m_x^2m_y^2m_z^2$$

$$\mathbf{E_0}(\mathbf{m}) = \frac{3}{2}\begin{bmatrix} \lambda_{100}(m_x^2 - \frac{1}{3}) & \lambda_{111} m_x m_y & \lambda_{111} m_x m_z \\ \lambda_{111} m_y m_x & \lambda_{100}(m_y^2 - \frac{1}{3}) & \lambda_{111} m_y m_z \\ \lambda_{111} m_z m_x & \lambda_{111} m_z m_y & \lambda_{100}(m_z^2 - \frac{1}{3}) \end{bmatrix}$$

5.1 Euler-Lagrange equations and the second variation

The constraint $|\mathbf{m}| = 1$ requires us to take variations of the sort, $\mathbf{m}_\varepsilon(\mathbf{x}) = \mathbf{R}_\varepsilon(\mathbf{x})\mathbf{m}_0(\mathbf{x})$, $\mathbf{R}_\varepsilon \in \mathrm{SO}(3)$.

We know,

$$\mathbf{R}_\varepsilon = \mathbf{I} + \varepsilon\mathbf{W} + \frac{1}{2}\varepsilon^2\mathbf{W}^2 + \cdots,$$

Here $\mathbf{W} \in M^{3\times3}_{antisymm}$, which is the set of all antisymmetric matrices, i.e. $\mathbf{W}^T = -\mathbf{W}$.

$\mathbf{u} = \mathbf{u}_0 + \varepsilon\mathbf{v}$

$\nabla\mathbf{u} = \nabla\mathbf{u}_0 + \varepsilon\nabla\mathbf{v}$

$\mathbf{E_s}(\mathbf{R}_\varepsilon\mathbf{m_0}) = \mathbf{E_s}(\mathbf{m_0}) + \varepsilon\dfrac{\partial\mathbf{E_s}}{\partial\mathbf{m}}(\mathbf{m_0})\mathbf{W}\mathbf{m_0} + \cdots$

Some expansions of terms in the micromagnetic energy:

$$|\nabla\mathbf{m}_\varepsilon|^2 = |\nabla\mathbf{m}_0|^2 + 2\varepsilon\nabla\mathbf{W}\mathbf{m}_0\cdot\nabla\mathbf{m}_0 + \varepsilon^2|\nabla\mathbf{W}\mathbf{m}_0|^2 + \cdots, \tag{5.6a}$$

$$\varphi(\mathbf{m}_\varepsilon) = \varphi(\mathbf{m}_0) + \varepsilon\frac{\partial\varphi(\mathbf{m}_0)}{\partial\mathbf{m}}\cdot\mathbf{W}\mathbf{m}_0 + \frac{\varepsilon^2}{2}\left[(\mathbf{W}\mathbf{m}_0)\cdot\frac{\partial^2\varphi(\mathbf{m}_0)}{\partial\mathbf{m}^2}(\mathbf{W}\mathbf{m}_0) + \frac{\partial\varphi(\mathbf{m}_0)}{\partial\mathbf{m}}\cdot\mathbf{W}^2\mathbf{m}_0\right] + \cdots, \tag{5.6b}$$

$$\mathbf{m}_\varepsilon\cdot\mathbf{h}_a = \mathbf{m}_0\cdot\mathbf{h}_a + \varepsilon\mathbf{W}\mathbf{m}_0\cdot\mathbf{h}_a + \frac{\varepsilon^2}{2}\mathbf{W}^2\mathbf{m}_0\cdot\mathbf{h}_a + \cdots, \tag{5.6c}$$

$$\frac{m_s^2}{8\pi}\int|\mathbf{h}_{\mathbf{m}_\varepsilon}|^2 = \frac{m_s^2}{8\pi}\int|\mathbf{h}_{\mathbf{m_0}}|^2 - m_s^2\varepsilon\int\mathbf{h}_{\mathbf{m_0}}\cdot\mathbf{W}\mathbf{m}_0 - \frac{m_s^2\,\varepsilon^2}{2}\int\mathbf{h}_{\mathbf{m_0}}\cdot\mathbf{W}^2\mathbf{m}_0 - \frac{m_s^2\,\varepsilon^2}{2}\int\mathbf{h}_1\cdot\mathbf{W}\mathbf{m}_0 + \cdots, \tag{5.6d}$$

In eqn.(5.6a), $\nabla\mathbf{W}\mathbf{m}_0\cdot\nabla\mathbf{m}_0 = W_{ij,k}m_{0\,j}m_{0\,i,k}$ and $|\nabla\mathbf{W}\mathbf{m}_0|^2 = W_{ij,k}m_{0\,j}W_{ip,k}m_{0\,p}$.

In eqn.(5.6d), the term $\mathbf{h}_1$ satisfies

$$\nabla\cdot(\mathbf{h}_1 + 4\pi\mathbf{W}\chi_\Omega\mathbf{m}_0) = 0 \tag{5.7}$$

$\mathbf{C}$ used above is fully symmetric as in linear elasticity, i.e. $C_{ijkl} = C_{klij} = C_{jikl} = C_{jilk}$.
The above implies,

$$\mathbf{C}\big[\mathbf{E}\big] : \mathbf{E} = \mathbf{C}\big[\mathbf{E}\big] : \nabla\mathbf{u} = \mathbf{C}\big[\nabla\mathbf{u}\big] : \mathbf{E} = \mathbf{C}\big[\nabla\mathbf{u}\big] : \nabla\mathbf{u} \tag{5.8}$$

$$\begin{aligned}
\mathbf{E}(\mathbf{u_0} + \varepsilon\mathbf{v}) &= \frac{\nabla\mathbf{u_0} + \varepsilon\nabla\mathbf{v} + \nabla^T\mathbf{u_0} + \varepsilon\nabla^T\mathbf{v}}{2} \\
&= \frac{\nabla\mathbf{u_0} + \nabla^T\mathbf{u_0}}{2} + \varepsilon\frac{\nabla\mathbf{v} + \nabla^T\mathbf{v}}{2} \\
&= \mathbf{E}(\mathbf{u_0}) + \varepsilon\mathbf{E}(\mathbf{v}) \\
&= \mathbf{E_0} + \varepsilon\mathbf{E_v}
\end{aligned}$$

Now we expand the elastic energy term,

$$\begin{aligned}
\frac{1}{2}\mathbf{C}\big[\mathbf{E} - \mathbf{E_s}(\mathbf{m})\big] : \big(\mathbf{E} - \mathbf{E_s}(\mathbf{m})\big) &= \frac{1}{2}\mathbf{C}\big[\mathbf{E}\big] : \mathbf{E} + \frac{\mathbf{1}}{\mathbf{2}}\mathbf{C}\big[\mathbf{E_s}(\mathbf{m})\big] : \mathbf{E_s}(\mathbf{m}) - \mathbf{C}\big[\mathbf{E}\big] : \mathbf{E_s}(\mathbf{m}). \\
&= \frac{1}{2}\mathbf{C}\big[\nabla\mathbf{u}\big] : \nabla\mathbf{u} + \frac{\mathbf{1}}{\mathbf{2}}\mathbf{C}\big[\mathbf{E_s}(\mathbf{m})\big] : \mathbf{E_s}(\mathbf{m}) - \mathbf{C}\big[\nabla\mathbf{u}\big] : \mathbf{E_s}(\mathbf{m})
\end{aligned}$$

$$\begin{aligned}
& L.H.S \\
= \;& \frac{1}{2}\mathbf{C}\big[\mathbf{E_0} + \varepsilon\mathbf{E_v}\big] : \big(\mathbf{E_0} + \varepsilon\mathbf{E_v}\big) - \mathbf{C}\big[\mathbf{E_0} + \varepsilon\mathbf{E_v}\big] : \Big(\mathbf{E_s}(\mathbf{m_0}) + \varepsilon\frac{\partial\mathbf{E_s}}{\partial\mathbf{m}}(\mathbf{m_0})\mathbf{W}\mathbf{m_0}\Big) \\
+ \;& \frac{1}{2}\mathbf{C}\big[\mathbf{E_s}(\mathbf{m_0}) + \varepsilon\frac{\partial\mathbf{E_s}}{\partial\mathbf{m}}(\mathbf{m_0})\mathbf{W}\mathbf{m_0}\big] : \Big(\mathbf{E_s}(\mathbf{m_0}) + \varepsilon\frac{\partial\mathbf{E_s}}{\partial\mathbf{m}}(\mathbf{m_0})\mathbf{W}\mathbf{m_0}\Big) + \cdots \\
= \;& \left\{\frac{1}{2}\mathbf{C}\big[\mathbf{E_0}\big] : \mathbf{E_0} + \frac{\mathbf{1}}{\mathbf{2}}\mathbf{C}\big[\mathbf{E_s}(\mathbf{m_0})\big] : \mathbf{E_s}(\mathbf{m_0}) - \mathbf{C}\big[\mathbf{E_0}\big] : \mathbf{E_s}(\mathbf{m_0})\right\} \\
+ \;& \varepsilon\left\{\mathbf{C}\big[\mathbf{E_0}\big] : \mathbf{E_v} + \mathbf{C}\big[\mathbf{E_s}(\mathbf{m_0})\big] : \frac{\partial\mathbf{E_s}}{\partial\mathbf{m}}(\mathbf{m_0})\mathbf{W}\mathbf{m_0} - \mathbf{C}\big[\mathbf{E_0}\big] : \frac{\partial\mathbf{E_s}}{\partial\mathbf{m}}(\mathbf{m_0})\mathbf{W}\mathbf{m_0} - \mathbf{C}\big[\mathbf{E_v}\big] : \mathbf{E_s}(\mathbf{m_0})\right\} \\
+ \;& \frac{\varepsilon^2}{2}\left\{\mathbf{C}\big[\mathbf{E_v}\big] : \mathbf{E_v} + \mathbf{C}\big[\frac{\partial\mathbf{E_s}}{\partial\mathbf{m}}\mathbf{W}\mathbf{m_0}\big] : \frac{\partial\mathbf{E_s}}{\partial\mathbf{m}}\mathbf{W}\mathbf{m_0} - \mathbf{2C}\big[\mathbf{E_v}\big] : \frac{\partial\mathbf{E_s}}{\partial\mathbf{m}}\mathbf{W}\mathbf{m_0}\right\} + \cdots
\end{aligned} \tag{5.9}$$

The first variation over $\mathbf{u}$ results in the following,

$$\int_\Omega \mathbf{C}\big[\mathbf{E_0} - \mathbf{E_s}(\mathbf{m_0})\big] : \mathbf{E_v} = \mathbf{0}$$

$$\int_\Omega \mathbf{C}\big[\mathbf{E_0} - \mathbf{E_s}(\mathbf{m_0})\big] : \nabla\mathbf{v} = \mathbf{0} \qquad \begin{cases} \forall \mathbf{v} \in H^1(\Omega, \mathbb{R}^3) \\ \cdots \text{ Use symmetry of } \mathbf{C} \text{ as in eqn.(5.8)} \end{cases} \tag{5.10}$$

The strong form of the above equation after integrating by parts is,

$$\nabla \cdot \mathbf{C}\big[\mathbf{E_0} - \mathbf{E_s}(\mathbf{m_0})\big]^T = 0 \tag{5.11}$$

with boundary condition being,

$$\mathbf{C}\big[\mathbf{E_0} - \mathbf{E_s}(\mathbf{m_0})\big]\mathbf{n} = \mathbf{0}$$

Now,

$$\begin{aligned} \mathbf{C}\big[\mathbf{E_0} - \mathbf{E_s}\big] : \frac{\partial \mathbf{E_s}}{\partial \mathbf{m}}(\mathbf{m_0})\mathbf{W}\mathbf{m_0} &= C_{ijkl}\big[E_{0\,ij} - E_{s\,ij}\big] \quad \Big(\frac{\partial E_{s\,kl}}{\partial m_p} W_{pq} m_{0\,q}\Big) \\ &= \mathbf{C}\big[\mathbf{E_0} - \mathbf{E_s}\big]\frac{\partial \mathbf{E_s}}{\partial \mathbf{m}}(\mathbf{m_0}) \;\cdot\; \mathbf{W}\mathbf{m_0} \end{aligned}$$

Using above result, first variation over $\mathbf{m}$ thus yields the Euler-Lagrange equations

$$\left(\frac{c}{R^2}\Delta\mathbf{m}_0 - \frac{\partial\varphi(\mathbf{m}_0)}{\partial\mathbf{m}} + m_s^2\mathbf{h}_a + m_s^2\mathbf{h}_{\mathbf{m_0}} + \mathbf{C}\big[\mathbf{E_0} - \mathbf{E_s}\big]\frac{\partial \mathbf{E_s}}{\partial \mathbf{m}}(\mathbf{m_0})\right) \times \mathbf{m}_0 = 0 \tag{5.12}$$

The natural boundary conditions are

$$(\nabla\mathbf{m}_0\,\mathbf{n}) \times \mathbf{m}_0 = 0 \quad \text{on } \partial\Omega \tag{5.13}$$

The second variation is

$$\begin{aligned} \frac{\partial^2}{\partial\varepsilon^2}\mathcal{E}(\mathbf{m}_\varepsilon, \mathbf{u}_\varepsilon)|_{\varepsilon=0} \;=\; & \int_\Omega \frac{c}{R^2}|\nabla\mathbf{W}\mathbf{m}_0|^2 + \mathbf{W}\mathbf{m}_0 \cdot \frac{\partial^2\varphi(\mathbf{m}_0)}{\partial\mathbf{m}^2}\mathbf{W}\mathbf{m}_0 + \frac{\partial\varphi(\mathbf{m}_0)}{\partial\mathbf{m}} \cdot \mathbf{W}^2\mathbf{m}_0 \\ & -m_s^2\mathbf{h}_a \cdot \mathbf{W}^2\,\mathbf{m}_0 - m_s^2\mathbf{h}_{\mathbf{m_0}}\mathbf{W}^2\mathbf{m}_0 - m_s^2\mathbf{h}_1 \cdot \mathbf{W}\mathbf{m}_0 + \mathbf{C}\big[\mathbf{E_v}\big] : \mathbf{E_v} \\ & +\mathbf{C}\big[\frac{\partial \mathbf{E_s}}{\partial \mathbf{m}}\,(\mathbf{m}_0)\mathbf{W}\mathbf{m_0}\big] : \frac{\partial \mathbf{E_s}}{\partial \mathbf{m}}(\mathbf{m_0})\mathbf{W}\mathbf{m_0} - \mathbf{2C}\big[\mathbf{E_v}\big] : \frac{\partial \mathbf{E_s}}{\partial \mathbf{m}}(\mathbf{m_0})\mathbf{W}\mathbf{m_0} \end{aligned} \tag{5.14}$$

Equations 5.11 and 5.12 form the complete set of equations which define the physics of magnetostriction under Brown's model. In the next sections we will investigate the possibility of choosing an appropriate solution 5.11 and 5.12 and check for the stability of this solution under change of certain parameters.

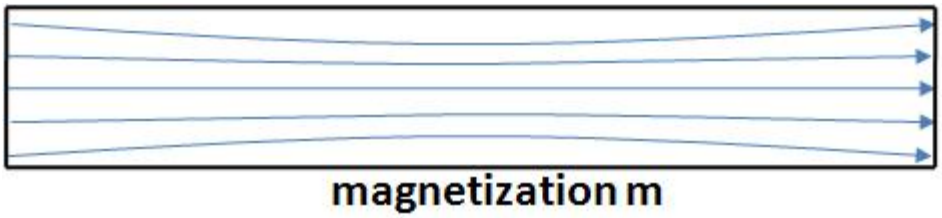

Figure 5.2: Flower domain in rectangular prisms, cylinder etc.

5.2 Galfenol nanowires and the "single domain states"

The galfenol wires made by electrodeposition are predominantly known to have a $\langle 110 \rangle$ orientation. Our aim in this section is to investigate whether galfenol wires in $\langle 110 \rangle$ orientation can have a starting state which is single domain. Since the work of Brown, it has been know that constant magnetization states, called single domain states are critical points for the micromagnetic energy in ellipsoids and all its limiting shapes. Brown investigated the stability of these states, and proposed a nucleation theory for breakdown of single domain states in ellipsoidal bodies.

In more recent years it has been observed that for various common shapes, e.g. cylinders, rectangular prisms etc, the approximation to a single domain state, called a flower pattern exists. Here the magnetization of the body is very nearly uniform except at the boundaries, where the competition between exchange, anisotropy and demag energy, causes the magnetization to bend slightly, so as to reduce the overall energy, by reducing the demag energy caused by surface charges. Numerical studies in micromagnetics also have calculated the energetics of these structures for e.g. in Schabes and Bertram [SB88]

The galfenol wires are long cylindrical shapes, with $\langle 110 \rangle$ orientation. To model then, we assume that they long thin prolate spheroids and are single domain along the wire axis. We than check for stability of the single domain state under perturbations in

the minor axis of the prolate spheroid. If Ω is an ellipsoid and $\mathbf{m}_0$ is constant on Ω,then $\mathbf{h_{m_0}}$ is constant on Ω. In that case (5.12) becomes,

$$\left(-\frac{\partial\varphi(\mathbf{m}_0)}{\partial\mathbf{m}} + m_s^2\mathbf{h}_a + m_s^2\mathbf{h_{m_0}} + \mathbf{C}\big[\nabla\mathbf{E_0} - \mathbf{E_s}\big]\frac{\partial\mathbf{E_s}}{\partial\mathbf{m}}(\mathbf{m_0})\right) \times \mathbf{m}_0 = 0$$

an algebraic restriction on the two constant vectors $\mathbf{m}_0, \mathbf{h}_a$ and $\dfrac{\partial\varphi(\mathbf{m}_0)}{\partial\mathbf{m}} \times \mathbf{m}_0$. It is satisfied for example if $\mathbf{h}_a = 0$ or in the same direction as $\mathbf{m}_0$, and the ellipsoid Ω is such that $\mathbf{h}_0$ is parallel to $\mathbf{m}_0$, e.g., when $\mathbf{m}_0$ is an eigenvector of the demagnetization matrix with additional restrictions on the crystallographic orientation of $\mathbf{m}_0$, due to the anisotropy term. Thus for e.g. $\mathbf{m}_0$ along $\langle 100\rangle, \langle 110\rangle$ and $\langle 111\rangle$ satisfies,

$$\frac{\partial\varphi(\mathbf{m}_0)}{\partial\mathbf{m}} \times \mathbf{m}_0 = 0$$

Now we examine the positivity of the second variation at this constant state. Choose an orthonormal basis $\mathbf{e}_1, \mathbf{e}_2, \mathbf{e}_3$ such that $\mathbf{m}_0 = \mathbf{e}_3$. In this basis, $\mathbf{W}$ has the form

$$\mathbf{W} = \begin{pmatrix} 0 & \alpha & \beta \\ -\alpha & 0 & \gamma \\ -\beta & -\gamma & 0 \end{pmatrix}. \tag{5.15}$$

Thus, in this basis $\mathbf{W}\mathbf{m}_0 = (\beta, \gamma, 0)$, and since $\mathbf{m}_0$ is constant we have that $\nabla\mathbf{W}\mathbf{m}_0 = \nabla(\mathbf{W}\mathbf{m}_0) = (\nabla\beta, \nabla\gamma, 0)$.

Also $\mathbf{m_0}$ being constant over Ω,makes $\mathbf{E_s}(\mathbf{m_0})$ constant, so that choosing $\mathbf{E_0} = \mathbf{E_s}$ satisfies (5.10) identically.

Now for $\mathbf{m_0}$ is constant,

$$\frac{\partial\mathbf{E_s}}{\partial\mathbf{m}}(\mathbf{m}_0)\mathbf{W}\mathbf{m_0} = \mathbf{E'_s}\mathbf{W}\mathbf{m_0} = \mathbf{E'_s}\begin{bmatrix}\beta\\ \gamma\\ 0\end{bmatrix}$$

where $\mathbf{E'_s}$ is a constant matrix independent of $x \in \Omega$.

Hence, using the first variation to simplify, the second variation becomes,

$$\begin{aligned}\frac{\partial^2}{\partial\varepsilon^2}\mathcal{E}(\mathbf{m}_\varepsilon,\mathbf{u}_\varepsilon)|_{\varepsilon=0} &= \int_\Omega \frac{c}{R^2}(|\nabla\beta|^2+|\nabla\gamma|^2)+\frac{\partial^2\varphi_0}{\partial m_1^2}\beta^2+2\frac{\partial^2\varphi_0}{\partial m_1\partial m_2}\beta\gamma+\frac{\partial^2\varphi_0}{\partial m_2^2}\gamma^2 \\ &- (\frac{\partial\varphi_0}{\partial m_3}-m_s h_{a\,3}-m_s^2 h_{0\,3})(\beta^2+\gamma^2)-(m_s^2 h_{1_1}\beta+m_s^2 h_{1_2}\gamma) \\ &+ \mathbf{C}\big[\mathbf{E_v}-\mathbf{E_s'}\mathbf{W}\mathbf{m_0}\big]:\big[\mathbf{E_v}-\mathbf{E_s'}\mathbf{W}\mathbf{m_0}\big] \qquad (5.16)\end{aligned}$$

Here,

$$h_{1_{i,i}}=-4\pi(\beta_{,1}+\gamma_{,2}),\quad h_{1_i}=-u_{,i}\,. \qquad (5.17)$$

(Note: this is full 3-D divergence of $\mathbf{h}_1$.)

Now let us define $\mathbf{Q}(\beta,\gamma,\mathbf{v})$ as the second variation given above.

$$\mathbf{Q}(\beta,\gamma,\mathbf{v})=\frac{\partial^{\mathbf{2}}}{\partial\varepsilon^{\mathbf{2}}}\mathcal{E}(\mathbf{m}_\varepsilon,\mathbf{u}_\varepsilon)|_{\varepsilon=\mathbf{0}}$$

For stability we need that $\mathbf{Q}(\beta,\gamma,\mathbf{v})$ is positive definite for all $\beta,\gamma,\mathbf{v}$.The minimum of $\mathbf{Q}(\beta,\gamma,\mathbf{v})$ w.r.t. $\beta,\gamma,\mathbf{v}$ must be just 0 for critical stability.

The bifurcation modes are thus given by,

$$(\mathcal{P})\qquad m=\inf_{(\beta,\gamma,\mathbf{v})\in\mathcal{A}}\mathbf{Q}(\beta,\gamma,\mathbf{v})\qquad \text{where } \mathcal{A}=H^1(\Omega,\mathbb{R})\times H^1(\Omega,\mathbb{R})\times H^1(\Omega,\mathbb{R}^3).$$

Let $\beta,\gamma,\mathbf{v}$ be minimizers of $\mathbf{Q}(\beta,\gamma,\mathbf{v})$. Taking variations on $\beta,\gamma,\mathbf{v}$.

$\beta_1=\beta+\varepsilon\delta\beta$

$\gamma_1=\gamma+\varepsilon\delta\gamma$

$\mathbf{v_1}=\mathbf{v}+\varepsilon\delta\mathbf{v}$

Thus we have $\mathbf{W}\mathbf{m_0}=\{\beta,\gamma,\mathbf{0}\}$ and $\mathbf{W_1}\mathbf{m_0}=\{\beta_1,\gamma_1,\mathbf{0}\}$

and $\mathbf{W_1}\mathbf{m_0}=\mathbf{W}\mathbf{m_0}+\varepsilon(\delta\mathbf{W}\mathbf{m_0})$, where $\delta\mathbf{W}\mathbf{m_0}=\begin{bmatrix}\delta\beta\\ \delta\gamma\\ 0\end{bmatrix}$

Variation for most terms can be calculates directly except a few terms for which we do this separate expansion.

$$\begin{aligned}\mathbf{C}\big[\mathbf{E}'_{\mathbf{s}}\mathbf{W_1}\mathbf{m_0}\big] : \mathbf{E}'_{\mathbf{s}}\mathbf{W_1}\mathbf{m_0} &= \mathbf{C}\big[\mathbf{E}'_{\mathbf{s}}\mathbf{W}\mathbf{m_0}\big] : \mathbf{E}'_{\mathbf{s}}\mathbf{W}\mathbf{m_0} + \mathbf{2}\varepsilon\mathbf{C}\big[\mathbf{E}'_{\mathbf{s}}\mathbf{W}\mathbf{m_0}\big] : \mathbf{E}'_{\mathbf{s}}\delta\mathbf{W}\mathbf{m_0} \\ &+ \varepsilon^2\mathbf{C}\big[\mathbf{E}'_{\mathbf{s}}\delta\mathbf{W}\mathbf{m_0}\big] : \mathbf{E}'_{\mathbf{s}}\delta\mathbf{W}\mathbf{m_0}\end{aligned}$$

$$\begin{aligned}-2\mathbf{C}\big[\mathbf{E}_{\mathbf{v_1}}\big] : \mathbf{E}'_{\mathbf{s}}\mathbf{W_1}\mathbf{m_0} &= -2\mathbf{C}\big[\mathbf{E}_{\mathbf{v}} + \varepsilon\mathbf{E}_{\delta\mathbf{v}}\big] : (\mathbf{E}'_{\mathbf{s}}\mathbf{W}\mathbf{m_0} + \varepsilon(\delta\mathbf{W}\mathbf{m_0})) \\ &= -2\mathbf{C}\big[\mathbf{E}_{\mathbf{v}}\big] : \mathbf{E}'_{\mathbf{s}}\mathbf{W}\mathbf{m_0} - \mathbf{2}\varepsilon\Big\{\mathbf{C}\big[\mathbf{E}_{\mathbf{v}}\big] : \mathbf{E}'_{\mathbf{s}}\delta\mathbf{W}\mathbf{m_0} \\ &\quad +\mathbf{C}\big[\mathbf{E}_{\delta\mathbf{v}}\big] : \mathbf{E}'_{\mathbf{s}}\mathbf{W}\mathbf{m_0}\Big\} - \mathbf{2}\varepsilon^{\mathbf{2}}\mathbf{C}\big[\mathbf{E}_{\delta\mathbf{v}}\big] : \mathbf{E}'_{\mathbf{s}}\delta\mathbf{W}\mathbf{m_0}\end{aligned}$$

Thus the first variation for $\mathbf{Q}$ is as follows:

$$\begin{aligned}\frac{\partial\mathbf{Q}}{\partial\varepsilon}|_{\varepsilon=0} &= \int_\Omega \frac{2c}{R^2}\{\nabla\beta_0.\nabla\delta\beta + \nabla\gamma_0.\nabla\delta\gamma\} + 2\frac{\partial^2\varphi_0}{\partial m_1^2}\beta_0\delta\beta + 2\frac{\partial^2\varphi_0}{\partial m_1\partial m_2}\beta_0\delta\gamma \\ &+2\frac{\partial^2\varphi_0}{\partial m_1\partial m_2}\delta\beta\gamma_0 + 2\frac{\partial^2\varphi_0}{\partial m_2^2}\gamma_0\delta\gamma - 2(m_s^2 h_{1_1}\delta\beta + m_s^2 h_{1_2}\delta\gamma) \\ &-2\{\frac{\partial\varphi_0}{\partial m_3} - m_s h_{a\,3} - m_s^2 h_{0\,3}\}(\beta_0\delta\beta + \gamma_0\delta\gamma) + 2\mathbf{C}\big[\mathbf{E}_{\mathbf{v}}\big] : \mathbf{E}_{\mathbf{v}} + \\ &2\mathbf{C}\big[\mathbf{E}'_{\mathbf{s}}\mathbf{W}\mathbf{m_0}\big] : \mathbf{E}'_{\mathbf{s}}\delta\mathbf{W}\mathbf{m_0} - \mathbf{2}\Big\{\mathbf{C}\big[\mathbf{E}_{\mathbf{v}}\big] : \mathbf{E}'_{\mathbf{s}}\delta\mathbf{W}\mathbf{m_0} + \mathbf{C}\big[\mathbf{E}_{\delta\mathbf{v}}\big] : \mathbf{E}'_{\mathbf{s}}\mathbf{W}\mathbf{m_0}\Big\}\end{aligned} \tag{5.18}$$

Now the Variation $\delta\mathbf{v}$ gives us that $\mathbf{v}$ satisfies:

$$\int_\Omega \mathbf{C}\big[\mathbf{E}_{\mathbf{v}} - \mathbf{E}'_{\mathbf{s}}\mathbf{W}\mathbf{m_0}\big] : \mathbf{E}_{\delta\mathbf{v}} = \mathbf{0} \qquad\qquad \forall\delta\mathbf{v} \in H^1(\Omega, \mathbb{R}^3) \tag{5.19}$$

If we choose $\delta\mathbf{v} = \mathbf{v}$ above, so we get,

$$\int_\Omega \mathbf{C}\big[\mathbf{E}_{\mathbf{v}} - \mathbf{E}'_{\mathbf{s}}\mathbf{W}\mathbf{m_0}\big] : \mathbf{E}_{\mathbf{v}} = \mathbf{0} \tag{5.20}$$

Using this relation eqn.(5.20), the equation for the bifurcation modes can be rewritten as minimizers β, γ of the a new functional $\mathbf{Q_1}$

$$\begin{aligned}
\inf_{(\beta,\gamma)\in\mathcal{A}_1} \mathbf{Q_1}(\beta,\gamma) &= \int_\Omega \frac{c}{R^2}(|\nabla\beta|^2+|\nabla\gamma|^2) + \frac{\partial^2\varphi_0}{\partial m_1^2}\beta^2 + 2\frac{\partial^2\varphi_0}{\partial m_1\partial m_2}\beta\gamma + \frac{\partial^2\varphi_0}{\partial m_2^2}\gamma^2 \\
&\quad - (\frac{\partial\varphi_0}{\partial m_3} - m_s h_{a\,3} - m_s^2 h_{0\,3})(\beta^2+\gamma^2) - (m_s^2 h_{1_1}\beta + m_s^2 h_{1_2}\gamma) \\
&+ \quad \mathbf{C}\big[\mathbf{E_v}\big] : \mathbf{E_v} + \mathbf{C}\big[\mathbf{E_s'Wm_0}\big] : \mathbf{E_s'Wm_0} - \mathbf{2C}\big[\mathbf{E_v}\big] : \mathbf{E_s'Wm_0}\,\mathbf{dx} \\
&= \int_\Omega \frac{c}{R^2}(|\nabla\beta|^2+|\nabla\gamma|^2) + \frac{\partial^2\varphi_0}{\partial m_1^2}\beta^2 + 2\frac{\partial^2\varphi_0}{\partial m_1\partial m_2}\beta\gamma + \frac{\partial^2\varphi_0}{\partial m_2^2}\gamma^2 \\
&\quad - (\frac{\partial\varphi_0}{\partial m_3} - m_s h_{a\,3} - m_s^2 h_{0\,3})(\beta^2+\gamma^2) - (m_s^2 h_{1\,1}\beta + m_s^2 h_{1\,2}\gamma) \\
&+ \quad \mathbf{C}\big[\mathbf{E_s'Wm_0}\big] : \mathbf{E_s'Wm_0} - \mathbf{C}\big[\mathbf{E_v}\big] : \mathbf{E_s'Wm_0} \\
&\quad \text{Using eqn.(5.20) above}
\end{aligned}$$

where $\mathbf{v}$ satisfies eqn.(5.19) and where, $\mathcal{A}_1 = H^1(\Omega,\mathbb{R}) \times H^1(\Omega,\mathbb{R})$.
Thus an alternate problem to,

$$(\mathcal{P}) \qquad m = \inf_{(\beta,\gamma,\mathbf{v})\in\mathcal{A}} \mathbf{Q}(\beta,\gamma,\mathbf{v}) = \frac{\partial^2}{\partial\varepsilon^2}\mathcal{E}(\mathbf{m}_\varepsilon, \mathbf{u}_\varepsilon)|_{\varepsilon=0}$$

is,

$$(\mathcal{P}_1) \qquad m = \inf_{(\beta,\gamma)\in\mathcal{A}_1} \mathbf{Q_1}(\beta,\gamma) \qquad \cdots \text{ with } \mathbf{v} \text{ satisfying eqn.(5.19)}$$

We will use either formulation as per requirement in the following sections.

5.3 Reduction of problem to simpler case

We use the second formulation as mentioned above where the bifurcation modes are given by problem $(\mathcal{P}_1)$,

$$\begin{aligned}
\inf_{(\beta,\gamma)\in\mathcal{A}_1} \mathbf{Q_1}(\beta,\gamma) &= \int_\Omega \frac{c}{R^2}(|\nabla\beta|^2+|\nabla\gamma|^2) + \begin{bmatrix}\beta\\ \gamma\end{bmatrix}\cdot\mathbf{K}\begin{bmatrix}\beta\\ \gamma\end{bmatrix} + \mathbf{N}(\beta,\gamma) \\
&+ \quad \mathbf{C}\big[\mathbf{E_s'Wm_0}\big] : \mathbf{E_s'Wm_0} - \mathbf{C}\big[\mathbf{E_v}\big] : \mathbf{E_s'Wm_0} \qquad (5.21)
\end{aligned}$$

$$\int_\Omega \mathbf{N}(\beta,\gamma) = -\int_\Omega (m_s^2 h_{1_1}\beta + m_s^2 h_{1_2}\gamma) = \frac{m_s^2}{4\pi}\int_{\mathbb{R}^3} |\mathbf{h_1}|^{\mathbf{2}}$$

with $\mathbf{v}$ solving for given $\mathbf{E_s'Wm_0}$,,

$$\int_\Omega \mathbf{C}\big[\mathbf{E_v} - \mathbf{E_s'Wm_0}\big] : \mathbf{E_w} = \mathbf{0} \qquad\qquad \forall \mathbf{w} \in \mathbf{H^1}(\mathbf{\Omega}, \mathbb{R}^{\mathbf{3}}) \tag{5.22}$$

or equivalently $\mathbf{v}$ minimizing

$$\inf_{\mathbf{v}\in\mathbf{H^1}(\mathbf{\Omega},\mathbb{R}^{\mathbf{3}})} I(\mathbf{v}+\varepsilon\delta\mathbf{v}) = \inf_{\mathbf{v}\in\mathbf{H^1}(\mathbf{\Omega},\mathbb{R}^{\mathbf{3}})} \int_{\mathbf{\Omega}} \frac{\mathbf{1}}{\mathbf{2}}\mathbf{C}\big[\mathbf{E_v} - \mathbf{E_s'Wm_0}\big] : (\mathbf{E_v} - \mathbf{E_s'Wm_0}) \tag{5.23}$$

We can check that eqn.(5.23) is equivalent to eqn.(5.22) by calculating the first variation for eqn.(5.23),

$$\frac{\partial I(\mathbf{v})}{\partial \varepsilon}|_{\varepsilon=0} = 2\int_\Omega \mathbf{C}\big[\mathbf{E_v} - \mathbf{E_s'Wm_0}\big] : \delta\mathbf{E} = \mathbf{0}$$

Also, if we call the elastic terms in $\mathbf{Q_1}$ as $\mathbf{E_{el}} = \int_{\mathbf{\Omega}} \mathbf{C}\big[\mathbf{E_s'Wm_0}\big] : \mathbf{E_s'Wm_0} - \mathbf{C}\big[\mathbf{E_v}\big] : \mathbf{E_s'Wm_0}$, we can check that $\mathbf{E_{el}} \geq \mathbf{0}$. To see that, choose $\mathbf{E_w} = \mathbf{E_v}$ in eqn.(5.22) to get,

$$\int_\Omega \mathbf{C}\big[\mathbf{E_v} - \mathbf{E_s'Wm_0}\big] : \mathbf{E_v} = \mathbf{0}$$

Adding this term to $\mathbf{E_{el}}$ we get,

$$\begin{aligned}
\mathbf{E_{el}} &= \mathbf{E_{el}} + \int_{\mathbf{\Omega}} \mathbf{C}\big[\mathbf{E_v} - \mathbf{E_s'Wm_0}\big] : \mathbf{E_v} = \mathbf{0} \\
&= \int_\Omega \mathbf{C}\big[\mathbf{E_s'Wm_0}\big] : \mathbf{E_s'Wm_0} - \mathbf{C}\big[\mathbf{E_v}\big] : \mathbf{E_s'Wm_0} + \int_{\mathbf{\Omega}} \mathbf{C}\big[\mathbf{E_v} - \mathbf{E_s'Wm_0}\big] : \mathbf{E_v} \\
&= \int_\Omega \mathbf{C}\big[\mathbf{E_v} - \mathbf{E_s'Wm_0}\big] : (\mathbf{E_v} - \mathbf{E_s'Wm_0}) \geq \mathbf{0} \qquad\qquad (5.24) \\
&\qquad \cdots \text{ As } \mathbf{C} \text{ is positive definite}
\end{aligned}$$

$\mathbf{N}(\beta,\gamma) = -(m_s^2 h_{1_1}\beta + m_s^2 h_{1_2}\gamma)$

Let us define

$$(\mathcal{P}^*_1) \qquad\qquad m^* = \inf_{(\beta^*,\gamma^*)\in\mathcal{A}_1^*} \mathbf{Q_1}(\beta,\gamma)$$

$$\mathcal{A}_1^* = \Big\{(\beta,\gamma) \in \mathcal{A}_1 : \int_\Omega \beta = \int_\Omega \gamma = 0\Big\}$$

.

Thus $\mathcal{A}_1^* \subset \mathcal{A}_1$ is a proper linear subspace. Thus,$m^* \geq m$.

We now show the reverse, i.e. $m \geq m^*$ and thus reduce the problem of solving $(\mathcal{P}_1)$ to solving $(\mathcal{P}^*{}_1)$.

To see that, let β, γ minimize $(\mathcal{P}_1)$, and let

$$\beta = \bar{\beta} + \hat{\beta} \text{ where } \bar{\beta} = \int_\Omega \beta$$

$$\gamma = \bar{\gamma} + \hat{\gamma} \text{ where } \bar{\gamma} = \int_\Omega \gamma$$

$$\mathbf{v} = \bar{\mathbf{v}} + \hat{\mathbf{v}} \text{ where } \bar{\mathbf{v}} = \int_{\mathbf{\Omega}} \mathbf{v}$$

By, the above definition, $(\hat{\beta}, \hat{\gamma}) \in \mathcal{A}^*{}_1$

We resolve different terms of $\mathbf{Q_1}(\beta, \gamma)$ using the above decomposition.

$$\int_\Omega \frac{c}{R^2}(|\nabla\tilde{\beta}|^2 + |\nabla\tilde{\gamma}|^2) = \int_\Omega \frac{c}{R^2}(|\nabla\hat{\beta}|^2 + |\nabla\hat{\gamma}|^2)$$

Since $(\hat{\beta}, \hat{\gamma}, \hat{\mathbf{v}}) \in \mathcal{A}_1^*$

$$\int_\Omega \begin{bmatrix}\hat{\beta}\\ \hat{\gamma}\end{bmatrix} \cdot \mathbf{K} \begin{bmatrix}\bar{\beta}\\ \bar{\gamma}\end{bmatrix} = \mathbf{K} \begin{bmatrix}\bar{\beta}\\ \bar{\gamma}\end{bmatrix} \cdot \int_{\mathbf{\Omega}} \begin{bmatrix}\hat{\beta}\\ \hat{\gamma}\end{bmatrix} = \begin{bmatrix}0\\ 0\end{bmatrix}$$

Since $\int_\Omega \mathbf{K} \begin{bmatrix}\hat{\beta}\\ \hat{\gamma}\end{bmatrix} = \mathbf{0}$,

$$\begin{aligned}\int_\Omega \begin{bmatrix}\beta\\ \gamma\end{bmatrix} \cdot \mathbf{K} \begin{bmatrix}\beta\\ \gamma\end{bmatrix} &= \int_\Omega \begin{bmatrix}\bar{\beta}\\ \bar{\gamma}\end{bmatrix} \cdot \mathbf{K} \begin{bmatrix}\bar{\beta}\\ \bar{\gamma}\end{bmatrix} + \begin{bmatrix}\hat{\beta}\\ \hat{\gamma}\end{bmatrix} \cdot \mathbf{K} \begin{bmatrix}\hat{\beta}\\ \hat{\gamma}\end{bmatrix} + \mathbf{2} \begin{bmatrix}\bar{\beta}\\ \bar{\gamma}\end{bmatrix} \cdot \mathbf{K} \begin{bmatrix}\hat{\beta}\\ \hat{\gamma}\end{bmatrix} \\ &= \int_\Omega \begin{bmatrix}\bar{\beta}\\ \bar{\gamma}\end{bmatrix} \cdot \mathbf{K} \begin{bmatrix}\bar{\beta}\\ \bar{\gamma}\end{bmatrix} + \begin{bmatrix}\hat{\beta}\\ \hat{\gamma}\end{bmatrix} \cdot \mathbf{K} \begin{bmatrix}\hat{\beta}\\ \hat{\gamma}\end{bmatrix}\end{aligned}$$

We know for ellipsoids,

$$\mathbf{N}(\beta, \gamma) = \mathbf{N}(\bar{\beta}, \bar{\gamma}) + \mathbf{N}(\hat{\beta}, \hat{\gamma})$$

To prove this, note that Maxwell's equation is linear. So if $\mathbf{m} = \bar{\mathbf{m}} + \hat{\mathbf{m}}$, then $\mathbf{h_m}$ can be split into $\bar{\mathbf{h}}_\mathbf{m} + \bar{\mathbf{h}}_\mathbf{m}$ where $\bar{\mathbf{h}}_\mathbf{m}$ and $\bar{\mathbf{h}}_\mathbf{m}$ solve Maxwell's equation for $\mathbf{m} = \bar{\mathbf{m}}$ and $\hat{\mathbf{m}}$ respectively. Now for ellipsoids for given constant vector field $\bar{\mathbf{m}}$, the corresponding $\bar{\mathbf{h}}_\mathbf{m}$ is constant and is given by $\bar{\mathbf{h}}_\mathbf{m} = \mathbf{D}\bar{\mathbf{m}} \quad \forall \mathbf{x} \in \boldsymbol{\Omega}$ with $\mathbf{D}$ being a constant matrix known as demagnetization tensor. Also let $\bar{\mathbf{h}}_\mathbf{m} = -\nabla \bar{u}_m$ for some $\bar{u}_m$. The weak form of Maxwell's equation can be written as,

$$\int_{\mathbb{R}^3} -\frac{1}{4\pi}\hat{\mathbf{h}}_\mathbf{m} \cdot \nabla\phi = \int_{\boldsymbol{\Omega}} \hat{\mathbf{m}} \cdot \nabla\phi \qquad \forall \text{ test functions } \phi : \mathbb{R}^\mathbf{3} \to \mathbb{R}$$

Choosing $\phi = \bar{u}_m$, we see that,

$$\int_{\mathbb{R}^3} -\frac{1}{4\pi}\hat{\mathbf{h}}_\mathbf{m} \cdot \nabla\bar{u}_m = \int_{\mathbb{R}^3} \frac{1}{4\pi}\hat{\mathbf{h}}_\mathbf{m} \cdot \bar{\mathbf{h}}_\mathbf{m} = \int_{\boldsymbol{\Omega}} \hat{\mathbf{m}} \cdot \nabla\bar{\mathbf{u}}_\mathbf{m} = -\int_{\boldsymbol{\Omega}} \hat{\mathbf{m}} \cdot \bar{\mathbf{h}}_\mathbf{m}$$

So,

$$\begin{aligned}
\mathbf{N}(\beta,\gamma) &= \frac{1}{4\pi}\int_{\mathbb{R}^3} |\mathbf{h_m}|^\mathbf{2} = \frac{\mathbf{1}}{\mathbf{4}\pi}\int_{\mathbb{R}^\mathbf{3}} |\bar{\mathbf{h}}_\mathbf{m} + \hat{\mathbf{h}}_\mathbf{m}|^\mathbf{2} \\
&= \frac{1}{4\pi}\int_{\mathbb{R}^3} |\bar{\mathbf{h}}_\mathbf{m}|^\mathbf{2} + \frac{\mathbf{1}}{\mathbf{4}\pi}\int_{\mathbb{R}^\mathbf{3}} |\hat{\mathbf{h}}_\mathbf{m}|^\mathbf{2} + \frac{\mathbf{1}}{\mathbf{2}\pi}\int_{\mathbb{R}^\mathbf{3}} \bar{\mathbf{h}}_\mathbf{m} \cdot \hat{\mathbf{h}}_\mathbf{m} \\
&= \frac{1}{4\pi}\int_{\mathbb{R}^3} |\bar{\mathbf{h}}_\mathbf{m}|^\mathbf{2} + \frac{\mathbf{1}}{\mathbf{4}\pi}\int_{\mathbb{R}^\mathbf{3}} |\hat{\mathbf{h}}_\mathbf{m}|^\mathbf{2} - \mathbf{2}\int_{\boldsymbol{\Omega}} \hat{\mathbf{m}} \cdot \bar{\mathbf{h}}_\mathbf{m} \\
&= \frac{1}{4\pi}\int_{\mathbb{R}^3} |\bar{\mathbf{h}}_\mathbf{m}|^\mathbf{2} + \frac{\mathbf{1}}{\mathbf{4}\pi}\int_{\mathbb{R}^\mathbf{3}} |\hat{\mathbf{h}}_\mathbf{m}|^\mathbf{2} - \mathbf{2D}\bar{\mathbf{m}} \cdot \int_{\boldsymbol{\Omega}} \hat{\mathbf{m}} \\
&= \frac{1}{4\pi}\int_{\mathbb{R}^3} |\bar{\mathbf{h}}_\mathbf{m}|^\mathbf{2} + \frac{\mathbf{1}}{\mathbf{4}\pi}\int_{\mathbb{R}^\mathbf{3}} |\hat{\mathbf{h}}_\mathbf{m}|^\mathbf{2} \\
&= \mathbf{N}(\bar{\beta},\bar{\gamma}) + \mathbf{N}(\hat{\beta},\hat{\gamma})
\end{aligned}$$

Next, $\mathbf{E}'_\mathbf{s}\mathbf{W}\mathbf{m_0} = \mathbf{E}'_\mathbf{s}\begin{bmatrix}\beta\\ \gamma\\ 0\end{bmatrix} = \mathbf{E}'_\mathbf{s}\begin{bmatrix}\bar{\beta}\\ \bar{\gamma}\\ 0\end{bmatrix} + \mathbf{E}'_\mathbf{s}\begin{bmatrix}\hat{\beta}\\ \hat{\gamma}\\ 0\end{bmatrix} = \mathbf{E}'_\mathbf{s}\mathbf{W}\bar{\mathbf{m}}_\mathbf{0} + \mathbf{E}'_\mathbf{s}\mathbf{W}\hat{\mathbf{m}}_\mathbf{0}$

while $\mathbf{E_v}$ solves

$$\int_\Omega \mathbf{C}\big[\mathbf{E_v} - \mathbf{E}'_\mathbf{s}\mathbf{W}\mathbf{m_0}\big] : \mathbf{E_w} = 0 \qquad \forall \mathbf{w} \in H^1(\Omega, \mathbb{R}^3)$$

By linearity of the above problem, we can choose $\mathbf{E_v} = \mathbf{E}_{\bar{\mathbf{v}}} + \mathbf{E}_{\hat{\mathbf{v}}}$, with $\mathbf{E}_{\bar{\mathbf{v}}}, \mathbf{E}_{\hat{\mathbf{v}}}$ respectively solving,

$$\int_\Omega \mathbf{C}\big[\mathbf{E}_{\bar{\mathbf{v}}} - \mathbf{E}'_\mathbf{s}\mathbf{W}\bar{\mathbf{m}}_\mathbf{0}\big] : \mathbf{E_w} = 0 \qquad \forall \mathbf{w} \in H^1(\Omega, \mathbb{R}^3) \tag{5.25}$$

$$\int_\Omega \mathbf{C}\big[\mathbf{E}_{\hat{\mathbf{v}}} - \mathbf{E}'_{\mathbf{s}}\mathbf{W}\hat{\mathbf{m}}_{\mathbf{0}}\big] : \mathbf{E}_{\mathbf{w}} = 0 \qquad\qquad \forall \mathbf{w} \in H^1(\Omega, \mathbb{R}^3) \tag{5.26}$$

Now, $\mathbf{E}'_{\mathbf{s}}\mathbf{W}\bar{\mathbf{m}}_{\mathbf{0}}$ being a constant matrix, we can choose $\bar{\mathbf{v}}$ to be an affine function, such that $\mathbf{E}_{\bar{\mathbf{v}}} = \mathbf{E}'_{\mathbf{s}}\mathbf{W}\bar{\mathbf{m}}_{\mathbf{0}}$ which solves eqn.(5.25) identically.
Set, $I = \mathbf{C}\big[\mathbf{E}'_{\mathbf{s}}\mathbf{W}\mathbf{m}_{\mathbf{0}}\big] : \mathbf{E}'_{\mathbf{s}}\mathbf{W}\mathbf{m}_{\mathbf{0}} - \mathbf{C}\big[\mathbf{E}_{\mathbf{v}}\big] : \mathbf{E}'_{\mathbf{s}}\mathbf{W}\mathbf{m}_{\mathbf{0}}$.

$$\begin{aligned}
I &= \mathbf{C}\big[\mathbf{E}'_{\mathbf{s}}\mathbf{W}\mathbf{m}_{\mathbf{0}} - \mathbf{E}_{\mathbf{v}}\big] : \mathbf{E}'_{\mathbf{s}}\mathbf{W}\mathbf{m}_{\mathbf{0}} \\
&= \mathbf{C}\big[\mathbf{E}'_{\mathbf{s}}\mathbf{W}\bar{\mathbf{m}}_{\mathbf{0}} + \mathbf{E}'_{\mathbf{s}}\mathbf{W}\hat{\mathbf{m}}_{\mathbf{0}} - \mathbf{E}_{\bar{\mathbf{v}}} - \mathbf{E}_{\hat{\mathbf{v}}}\big] : (\mathbf{E}'_{\mathbf{s}}\mathbf{W}\bar{\mathbf{m}}_{\mathbf{0}} + \mathbf{E}'_{\mathbf{s}}\mathbf{W}\hat{\mathbf{m}}_{\mathbf{0}}) \\
&= \mathbf{C}\big[\mathbf{E}'_{\mathbf{s}}\mathbf{W}\bar{\mathbf{m}}_{\mathbf{0}} - \mathbf{E}_{\bar{\mathbf{v}}}\big] : \mathbf{E}'_{\mathbf{s}}\mathbf{W}\bar{\mathbf{m}}_{\mathbf{0}} + \mathbf{C}\big[\mathbf{E}'_{\mathbf{s}}\mathbf{W}\hat{\mathbf{m}}_{\mathbf{0}} - \mathbf{E}_{\hat{\mathbf{v}}}\big] : \mathbf{E}'_{\mathbf{s}}\mathbf{W}\hat{\mathbf{m}}_{\mathbf{0}} + \mathbf{C}\big[\mathbf{E}'_{\mathbf{s}}\mathbf{W}\bar{\mathbf{m}}_{\mathbf{0}} \\
&\quad -\mathbf{E}_{\bar{\mathbf{v}}}\big] : \mathbf{E}'_{\mathbf{s}}\mathbf{W}\hat{\mathbf{m}}_{\mathbf{0}} + \mathbf{C}\big[\mathbf{E}'_{\mathbf{s}}\mathbf{W}\hat{\mathbf{m}}_{\mathbf{0}} - \mathbf{E}_{\hat{\mathbf{v}}}\big] : \mathbf{E}'_{\mathbf{s}}\mathbf{W}\bar{\mathbf{m}}_{\mathbf{0}} \\
&= \mathbf{C}\big[\mathbf{E}'_{\mathbf{s}}\mathbf{W}\hat{\mathbf{m}}_{\mathbf{0}} - \mathbf{E}_{\hat{\mathbf{v}}}\big] : \mathbf{E}'_{\mathbf{s}}\mathbf{W}\hat{\mathbf{m}}_{\mathbf{0}} + \mathbf{C}\big[\mathbf{E}'_{\mathbf{s}}\mathbf{W}\hat{\mathbf{m}}_{\mathbf{0}} - \mathbf{E}_{\hat{\mathbf{v}}}\big] : \mathbf{E}'_{\mathbf{s}}\mathbf{W}\bar{\mathbf{m}}_{\mathbf{0}} \\
&\qquad\qquad \cdots \quad \because \mathbf{E}_{\bar{\mathbf{v}}} = \mathbf{E}'_{\mathbf{s}}\mathbf{W}\bar{\mathbf{m}}_{\mathbf{0}} \\
&= \mathbf{C}\big[\mathbf{E}'_{\mathbf{s}}\mathbf{W}\hat{\mathbf{m}}_{\mathbf{0}} - \mathbf{E}_{\hat{\mathbf{v}}}\big] : \mathbf{E}'_{\mathbf{s}}\mathbf{W}\hat{\mathbf{m}}_{\mathbf{0}} \\
&\qquad\qquad\qquad \cdots \quad \text{Choosing } \mathbf{E}_{\mathbf{w}} = \mathbf{E}'_{\mathbf{s}}\mathbf{W}\bar{\mathbf{m}}_{\mathbf{0}} \text{ in eqn(5.25)}
\end{aligned}$$

$$\begin{aligned}
\mathbf{Q_1}(\beta,\gamma) &= \int_\Omega \frac{c}{R^2}(|\nabla\beta|^2 + |\nabla\gamma|^2) + \begin{bmatrix}\beta\\ \gamma\end{bmatrix} \cdot \mathbf{K} \begin{bmatrix}\beta\\ \gamma\end{bmatrix} + \mathbf{N}(\beta,\gamma) + \mathbf{C}\big[\mathbf{E}'_{\mathbf{s}}\mathbf{W}\mathbf{m}_{\mathbf{0}}\big] : \mathbf{E}'_{\mathbf{s}}\mathbf{W}\mathbf{m}_{\mathbf{0}} \\
&\quad -\mathbf{C}\big[\mathbf{E}_{\mathbf{v}}\big] : \mathbf{E}'_{\mathbf{s}}\mathbf{W}\mathbf{m}_{\mathbf{0}} \\
&= \int_\Omega \frac{c}{R^2}(|\nabla\hat{\beta}|^2 + |\nabla\hat{\gamma}|^2) + \begin{bmatrix}\hat{\beta}\\ \hat{\gamma}\end{bmatrix} \cdot \mathbf{K} \begin{bmatrix}\hat{\beta}\\ \hat{\gamma}\end{bmatrix} + \mathbf{N}(\hat{\beta},\hat{\gamma}) + \mathbf{C}\big[\mathbf{E}'_{\mathbf{s}}\mathbf{W}\hat{\mathbf{m}}_{\mathbf{0}} - \mathbf{E}_{\hat{\mathbf{v}}}\big] : \mathbf{E}'_{\mathbf{s}}\mathbf{W}\hat{\mathbf{m}}_{\mathbf{0}} \\
&\quad +\Big(\mathbf{N}(\bar{\beta},\bar{\gamma}) + \begin{bmatrix}\bar{\beta}\\ \bar{\gamma}\end{bmatrix} \cdot \mathbf{K} \begin{bmatrix}\bar{\beta}\\ \bar{\gamma}\end{bmatrix}\Big) \\
&= \mathbf{Q_1}(\hat{\beta},\hat{\gamma}) + \Big(\mathbf{N}(\bar{\beta},\bar{\gamma}) + \begin{bmatrix}\bar{\beta}\\ \bar{\gamma}\end{bmatrix} \cdot \mathbf{K} \begin{bmatrix}\bar{\beta}\\ \bar{\gamma}\end{bmatrix}\Big) \\
&\geq \mathbf{Q_1}(\hat{\beta},\hat{\gamma})
\end{aligned} \tag{5.27}$$

$$\Big\{ \because \forall \text{ constant } (\bar{\beta},\bar{\gamma}), \quad \mathbf{N}(\bar{\beta},\bar{\gamma}) + \begin{bmatrix}\bar{\beta}\\ \bar{\gamma}\end{bmatrix} \cdot \mathbf{K} \begin{bmatrix}\bar{\beta}\\ \bar{\gamma}\end{bmatrix} \geq \mathbf{0} \Big\}$$

Thus, $\inf_{(\beta,\gamma)\in\mathcal{A}_1} \mathbf{Q_1}(\beta,\gamma) \geq \inf_{(\bar{\beta},\bar{\gamma})\in\mathcal{A}_1^*} \mathbf{Q_1}(\hat{\beta},\hat{\gamma})$
Thus we have proved the reverse i.e. $m \geq m^*$. So $m = m^*$ and we can now solve the reduced problem $(\mathcal{P}^*{}_1)$ $m^* = \inf_{(\beta^*,\gamma^*)\in\mathcal{A}_1^*} \mathbf{Q_1}(\beta,\gamma)$

5.4 Existence of and Lower Bound for Critical Radius

We have reduced the problem to the following:

$$(\mathcal{P}^*{}_1) \qquad m^* = \inf_{(\beta,\gamma)\in\mathcal{A}_1^*} \mathbf{Q_1}(\beta,\gamma) \tag{5.28}$$

$$= \inf_{(\beta,\gamma)\in\mathcal{A}_1^*} \int_\Omega \frac{c}{R^2}(|\nabla\beta|^2 + |\nabla\gamma|^2) + \begin{bmatrix}\beta\\ \gamma\end{bmatrix} \cdot \mathbf{K} \begin{bmatrix}\beta\\ \gamma\end{bmatrix} + \mathbf{N}(\beta,\gamma)$$
$$+\mathbf{C}\big[\mathbf{E_s'Wm_0}\big] : \mathbf{E_s'Wm_0} - \mathbf{C}\big[\mathbf{E_v}\big] : \mathbf{E_s'Wm_0}\,\mathbf{dx} \tag{5.29}$$

$\mathbf{v}$ minimizing for given $\mathbf{E_s'Wm_0}$,

$$\inf_{\mathbf{w}\in H^1(\Omega,\mathbb{R}^3)} \int_\Omega \frac{1}{2}\mathbf{C}\big[\mathbf{E_v} - \mathbf{E_s'Wm_0}\big] : (\mathbf{E_v} - \mathbf{E_s'Wm_0})$$

We now calculate the exact forms of all other terms in the minimization problem above. For the Galfenol wire with $\langle 110\rangle$ wire orientation, we have

$$\mathbf{K} = \begin{bmatrix} -2K_1 - N_z {m_s}^2 & 0 \\ 0 & K_1 - N_z {m_s}^2 \end{bmatrix} = \begin{bmatrix} K_{11} & 0 \\ 0 & K_{22} \end{bmatrix}$$

For (x,y,z), with x along $\langle 010\rangle$ direction, y along $\langle 001\rangle$ and z along $\langle 100\rangle$,

$$\mathbf{E_s} = \begin{bmatrix} \frac{3}{2}\lambda_{100}(m_1 * m_1 - \frac{1}{3}) & \frac{3}{2}\lambda_{111}m_1m_2 & \frac{3}{2}\lambda_{111}m_1m_3 \\ \frac{3}{2}\lambda_{111}m_2m_1 & \frac{3}{2}\lambda_{100}(m_2 * m_2 - \frac{1}{3}) & \frac{3}{2}\lambda_{111}m_2m_3 \\ \frac{3}{2}\lambda_{111}m_3m_1 & \frac{3}{2}\lambda_{111}m_3m_2 & \frac{3}{2}\lambda_{100}(m_3 * m_3 - \frac{1}{3}) \end{bmatrix}$$

with (m_1,m_2,m_3) direction cosines of $\mathbf{m}$ along (x,y,z) directions. We rotate the coordinate system so that (x,y,z) is along $\langle\bar{1}10\rangle, \langle 001\rangle, \langle 110\rangle$ direction respectively, then E_s in the new system becomes,

$$\mathbf{E_s(m)} = \mathbf{R_0^T E_s R_0} \qquad \cdots \quad \mathbf{R_0} \in \mathbf{SO(3)} \quad \text{corresponding to coordinate transformation}$$
$$= \begin{bmatrix} \frac{\left(-6\lambda_{111}m_1m_3+\lambda_{100}\left(-2+3m_1^2+3m_3^2\right)\right)}{4} & \frac{3\lambda_{111}m_2(m_1-m_3)}{2\sqrt{2}} & \frac{3\lambda_{100}\left(m_1^2-m_3^2\right)}{4} \\ \frac{3\lambda_{111}m_2(m_1-m_3)}{2\sqrt{2}} & \frac{\lambda_{100}\left(-1+3m_2^2\right)}{2} & \frac{3\lambda_{111}m_2(m_1+m_3)}{2\sqrt{2}} \\ \frac{3\lambda_{100}\left(m_1^2-m_3^2\right)}{4} & \frac{3\lambda_{111}m_2(m_1+m_3)}{2\sqrt{2}} & \frac{\left(6\lambda_{111}m_1m_3+\lambda_{100}\left(-2+3m_1^2+3m_3^2\right)\right)}{4} \end{bmatrix}$$

In new coordinate system, if the direction cosines of $\mathbf{m}$ are given by (l, m, n)
$m_1 = \frac{l+n}{\sqrt{2}}$, $m_3 = \frac{n-l}{\sqrt{2}}$ and $m_2 = m$.
Using these relations,

$$\mathbf{E_s}(l,m,n) = \begin{bmatrix} \frac{\left(3\lambda_{111}(l^2-n^2)+\lambda_{100}\left(-2+3l^2+3n^2\right)\right)}{4} & \frac{3\lambda_{111}ml}{2} & 3\lambda_{100}nl \\ \frac{3\lambda_{111}ml}{2} & \frac{\lambda_{100}\left(-1+3m^2\right)}{2} & \frac{3\lambda_{111}mn}{2} \\ 3\lambda_{100}ln & \frac{3\lambda_{111}mn}{2} & \frac{\left(3\lambda_{111}(n^2-l^2)+\lambda_{100}\left(-2+3l^2+3n^2\right)\right)}{4} \end{bmatrix} \quad (5.30)$$

$\mathbf{m_0}$ in the (l, m, n) system is $(0, 0, 1)$, and thus $\mathbf{W}\mathbf{m_0} = (\beta, \gamma, \mathbf{0})$.

$$\frac{\partial \mathbf{E_s}}{\partial l}(\mathbf{m_0}) = \begin{bmatrix} \frac{6\lambda_{111}l+6\lambda_{100}l}{4} & \frac{3\lambda_{111}m}{2} & 3\lambda_{100}n \\ \frac{3\lambda_{111}m}{2} & 0 & 0 \\ 3\lambda_{100}n & 0 & \frac{-6\lambda_{111}l+6\lambda_{100}l}{4} \end{bmatrix} = \begin{bmatrix} 0 & 0 & 3\lambda_{100} \\ 0 & 0 & 0 \\ 3\lambda_{100} & 0 & 0 \end{bmatrix}$$

$$\frac{\partial \mathbf{E_s}}{\partial m}(\mathbf{m_0}) = \begin{bmatrix} 0 & \frac{3\lambda_{111}l}{2} & 0 \\ \frac{3\lambda_{111}l}{2} & 3\lambda_{100}m & \frac{3\lambda_{111}n}{2} \\ 0 & \frac{3\lambda_{111}n}{2} & 0 \end{bmatrix} = \begin{bmatrix} 0 & 0 & 0 \\ 0 & 0 & \frac{3\lambda_{111}}{2} \\ 0 & \frac{3\lambda_{111}}{2} & 0 \end{bmatrix}$$

Thus

$$\frac{\partial \mathbf{E_s}}{\partial \mathbf{m}}(\mathbf{m_0})\mathbf{W}\mathbf{m_0} = \begin{bmatrix} 0 & 0 & 3\lambda_{100}\beta \\ 0 & 0 & \frac{3\lambda_{111}}{2}\gamma \\ 3\lambda_{100}\beta & \frac{3\lambda_{111}}{2}\gamma & 0 \end{bmatrix}$$

Now, in the above expression for $\mathbf{Q_1}(\beta, \gamma, \mathbf{v})$, the only negative definite term comes from the $\begin{bmatrix}\beta \\ \gamma\end{bmatrix} \cdot \mathbf{K} \begin{bmatrix}\beta \\ \gamma\end{bmatrix}$ term. All the other terms are positive definite.From Poincare Inequality for Admissible Space $\mathcal{A}^*$, we know that,

$$\int_\Omega (\beta^2 + \gamma^2) \leq \lambda(\Omega) \int_\Omega (|\nabla\beta|^2 + |\nabla\gamma|^2)$$

with $\lambda(\Omega)$ is the Poincare constant
For given Ω which is a prolate spheroid with major axis q which is also the aspect ratio of spheroid, because of the rescaling of the domain we did earlier. The Poincare constant for such Ω, (which is also the smallest eigenvalue of the Laplace operator on Ω) has dependence as follows, $\lambda(\Omega) = \frac{c_1}{q^2}$ where c_1 is a constant.

Thus, for given Ω, and $\lambda(\Omega) = \frac{c_1}{q^2}$, the 1st term of $\mathbf{Q}(\beta, \gamma, \mathbf{v})$ is,

$$\int_\Omega \frac{c}{R^2}(|\nabla\beta|^2 + |\nabla\gamma|^2) \geq \Big(\frac{1}{R^2}\Big)\Big(\frac{cc_1}{q^2}\Big)\int_\Omega (|\beta|^2 + |\gamma|^2) = \Big(\frac{1}{R^2}\Big)\Big(\frac{cc_1}{q^2}\Big)\Big(\|\beta\|_{L^2} + \|\gamma\|_{L^2}\Big)$$

Thus choosing R, really small, we can always make $Q(\beta, \gamma, \mathbf{v})$ positive, for any choice of $(\beta, \gamma, \mathbf{v}) \in \mathcal{A}^*$ as all other terms are bounded by some constant times the L^2 norm of (β, γ). Beginning from a small enough R, as we increase R, we look for the smallest such $R = R_{cr}$, such that for some choice of $(\beta, \gamma, \mathbf{v})$ (not necessarily unique), $\mathbf{Q_1}$ changes sign from positive to negative through 0.

The problem $\mathcal{P}_1^*$ gives a solution to above problem and it can alternately also be stated as a minimization problem of its Rayleigh quotient,

$$R_{cr}^2 = \inf_{(\beta,\gamma)\in\mathcal{A}_1^*} \frac{\displaystyle\int_\Omega c(|\nabla\beta|^2 + |\nabla\gamma|^2)\, d\mathbf{x}}{\displaystyle\int_\Omega -\begin{bmatrix}\beta\\ \gamma\end{bmatrix}\cdot\mathbf{K}\begin{bmatrix}\beta\\ \gamma\end{bmatrix} - \mathbf{N}(\beta,\gamma) - \mathbf{C}\big[\mathbf{E_s'Wm_0} - \mathbf{E_v}\big] : \mathbf{E_s'Wm_0}\, \mathbf{dx}}$$

where the R.H.S is the Rayleigh Quotient for the problem $\mathcal{P}_1^*$.

Now. let us define a new problem,

$$(\mathcal{P}_1^{**}) \qquad m^{**} = \inf_{(\beta,\gamma)\in\mathcal{A}_1^*} \int_\Omega \frac{c}{R^2}(|\nabla\beta|^2 + |\nabla\gamma|^2) + \begin{bmatrix}\beta\\ \gamma\end{bmatrix}\cdot\mathbf{K}\begin{bmatrix}\beta\\ \gamma\end{bmatrix}\, \mathbf{dx}$$

By using the same argument, involving Poincare Inequality on $\mathcal{A}_1^*$, we can prove the existence of a critical radius which we call R_{lb} and $(\beta_2, \gamma_2) \in \mathcal{A}^*$, which gives this critical radius. As mentioned above an equivalent problem to $\mathcal{P}_\infty^{**}$ is to minimizes its Rayleigh Quotient,

$$R_{lb}^2 = \inf_{(\beta,\gamma)\in\mathcal{A}_1^*} \frac{\displaystyle\int_\Omega c(|\nabla\beta|^2 + |\nabla\gamma|^2)\, d\mathbf{x}}{\displaystyle\int_\Omega -\begin{bmatrix}\beta\\ \gamma\end{bmatrix}\cdot\mathbf{K}\begin{bmatrix}\beta\\ \gamma\end{bmatrix}}$$

We will now prove that R_{lb} forms a lower bound to R_{cr}. To see that we only need to compare the Rayleigh quotients corresponding to the two radii. Note that the elastic and magnetic terms in $\mathbf{Q_1}$ are positive, $\mathbf{N}(\beta,\gamma)+\mathbf{C}\big[\mathbf{E_s'Wm_0}-\mathbf{E_v}\big]:\mathbf{E_s'Wm_0}\geq\mathbf{0}$ from eqn.(5.24) and positivity of the magnetostatic energy.

Thus $\forall(\beta,\gamma)$,

$$\frac{\displaystyle\int_\Omega c(|\nabla\beta|^2+|\nabla\gamma|^2)\,d\mathbf{x}}{\displaystyle\int_\Omega -\begin{bmatrix}\beta\\ \gamma\end{bmatrix}\cdot\mathbf{K}\begin{bmatrix}\beta\\ \gamma\end{bmatrix}} \leq \frac{\displaystyle\int_\Omega c(|\nabla\beta|^2+|\nabla\gamma|^2)\,d\mathbf{x}}{\displaystyle\int_\Omega -\begin{bmatrix}\beta\\ \gamma\end{bmatrix}\cdot\mathbf{K}\begin{bmatrix}\beta\\ \gamma\end{bmatrix}-\mathbf{N}(\beta,\gamma)-\mathbf{C}\big[\mathbf{E_s'Wm_0}-\mathbf{E_v}\big]:\mathbf{E_s'Wm_0}\,\mathbf{dx}}$$

Thus taking infimum on both sides, $R_{lb}^2\leq R_{cr}^2$.

Thus, the critical radius R_{lb}^2, forms a lower bound for the actual critical radius, R_{cr}^2

Now note that in the minimization,

$$(\mathcal{P}^{**})\qquad m^{**} = \inf_{(\beta,\gamma)\in\mathcal{A}_1^*}\int_\Omega \frac{c}{R^2}(|\nabla\beta|^2+|\nabla\gamma|^2)+\begin{bmatrix}\beta\\ \gamma\end{bmatrix}\cdot\mathbf{K}\begin{bmatrix}\beta\\ \gamma\end{bmatrix}\,\mathbf{dx}$$

$$\text{with }\mathbf{K}=\begin{bmatrix}-2K_1-N_z{m_s}^2 & 0\\ 0 & K_1-N_z{m_s}^2\end{bmatrix}$$

$(-2K_1-N_z{m_s}^2)<(K_1-N_z{m_s}^2)$ Using similar arguments as above, we can see that the problem,

$$\inf\Big\{\int_\Omega \frac{c}{R^2}(|\nabla\beta|^2)+(-2K_1-N_z{m_s}^2)|\beta|^2\Big\}$$

gives R_{LB} which forms a lower bound to R_{cr}.

So for a lower bound radius we solve $\inf\Big\{\displaystyle\int_\Omega \frac{c}{R^2}(|\nabla\beta|^2)+(-2K_1-N_z{m_s}^2)|\beta|^2\Big\}$.

5.5 Calculation of R_{LB}

For calculation of R_{LB}, we need solution to problem,

$$\inf_{\beta\in\mathcal{A}_1^*}\int_\Omega \frac{c}{R^2}|\nabla\beta|^2+K_{11}\beta^2\,d\mathbf{x}=0$$

The Euler Lagrange equation for above problem is given by,

$$\Delta\beta - K_{11}R^2\beta = 0 \qquad \text{in} \qquad \Omega$$

with the Boundary Condition,

$$\frac{d\beta}{dn} = 0 \qquad \text{on} \qquad \partial\Omega \qquad \{ \text{ n is unit normal } \}$$

We use prolate spheroidal coordinates (ξ, η, θ).

$$\frac{1}{a^2(\xi^2-\eta^2)}\Big\{\frac{\partial}{\partial\xi}\big[(\xi^2-1)\frac{\partial\beta}{\partial\xi}\big]+\big[\frac{\partial}{\partial\eta}\big[(1-\eta^2)\frac{\partial\beta}{\partial\eta}\big]\Big\}+\frac{1}{a^2(\xi^2-1)(1-\eta^2)}\frac{\partial^2\beta}{\partial\theta^2}-K_{11}R^2\beta = 0 \tag{5.31}$$

For more on these coordinate systems refer to Flammer [Fla57]. In the notation used above a is half the distance between the foci of the prolate spheroid. Now, for β we choose a partial fourier series as follows:

$$\beta(\xi,\eta,\theta) = \sum_{k=0}^{N} A_k(\xi,\eta)\sin(k\theta-\theta_k) \qquad \text{B.C.gives } \frac{\partial A_k}{\partial\xi}(\xi_0) = 0 \tag{5.32}$$

Note the domain is decomposable in prolate spheroidal coordinates as follows:

$$\Omega = \Omega' \times [0, 2\pi] \qquad \text{with} = \Omega' = (1, \xi_0) \times (-1, 1)$$

$\beta \in \mathcal{A}_1^* \Rightarrow \beta \in W^{1,2}(\Omega), \quad \int_\Omega \beta = 0.$ Thus,from Fourier representation of β eqn.(5.32) we get,

$$||\beta||_{L^2}^2 = \sum_{k=0}^{N}\int_{\Omega'}|A_k|^2 < +\infty \tag{5.33}$$

$$||\nabla\beta||_{L^2}^2 = \frac{1}{a^2}\sum_{k=0}^{N}\int_{\Omega'}\Big(\frac{\xi^2-1}{\xi^2-\eta^2}\Big)|\frac{\partial A_k}{\partial\xi}|^2+\Big(\frac{1-\eta^2}{\xi^2-\eta^2}\Big)|\frac{\partial A_k}{\partial\eta}|^2+\Big(\frac{k^2}{(\xi^2-1)(1-\eta^2)}\Big)|A_k|^2 < +\infty \tag{5.34}$$

Substituting the form of β in the equation 5.31 above we get,

$$\frac{1}{a^2(\xi^2-\eta^2)}\Big\{\frac{\partial}{\partial\xi}\big[(\xi^2-1)\frac{\partial A_k}{\partial\xi}\big]+\big[\frac{\partial}{\partial\eta}\big[(1-\eta^2)\frac{\partial A_k}{\partial\eta}\big]\Big\}-\frac{k^2}{a^2(\xi^2-1)(1-\eta^2)}A_k = K_{11}R^2A_k \tag{5.35}$$

Multiplying above by A_k and integrating over Ω' followed by integration by parts we get,

$$R^2 = \frac{\int_{\Omega'}\left(\frac{\xi^2-1}{\xi^2-\eta^2}\right)|\frac{\partial A_k}{\partial\xi}|^2+\left(\frac{1-\eta^2}{\xi^2-\eta^2}\right)|\frac{\partial A_k}{\partial\eta}|^2+\int_{\Omega'}\left(\frac{k^2}{(\xi^2-1)(1-\eta^2)}\right)|A_k|^2}{a^2\int_{\Omega'}K_{11}|A_k|^2}$$

We compare such solutions β to a test solution of the form $\beta_0 = A_{00}(\xi,\eta)$, i.e. independent of θ.

Then, if (β_0, R_{00}) is to be a solution to 5.31, A_{00}, has to satisfy,

$$\Delta' A_{00} = K_{11}R_{00}^2A_{00}, \qquad \Delta' = \frac{1}{a^2(\xi^2-\eta^2)}\Big\{\frac{\partial}{\partial\xi}\big[(\xi^2-1)\frac{\partial}{\partial\xi}\big]+\big[\frac{\partial}{\partial\eta}\big[(1-\eta^2)\frac{\partial}{\partial\eta}\big]\Big\} \tag{5.36}$$

Given this test solution we try to get best possible R_{00} by choosing,

$$R_{00} = \inf\frac{\int_{\Omega'}\left(\frac{\xi^2-1}{\xi^2-\eta^2}\right)|\frac{\partial A_{00}}{\partial\xi}|^2+\left(\frac{1-\eta^2}{\xi^2-\eta^2}\right)|\frac{\partial A_{00}}{\partial\eta}|^2}{a^2\int_{\Omega'}K_{11}|A_{00}|^2} \qquad \text{where } A_{00} \text{ satisfies eqn.(5.33),(5.34)}$$

Thus we see that,

$$\begin{aligned}
R^2 &= \frac{\int_{\Omega'}\left(\frac{\xi^2-1}{\xi^2-\eta^2}\right)|\frac{\partial A_k}{\partial\xi}|^2+\left(\frac{1-\eta^2}{\xi^2-\eta^2}\right)|\frac{\partial A_k}{\partial\eta}|^2+\int_{\Omega'}\left(\frac{k^2}{(\xi^2-1)(1-\eta^2)}\right)|A_k|^2}{a^2\int_{\Omega'}K_{11}|A_k|^2} \\
&\geq \frac{\int_{\Omega'}\left(\frac{\xi^2-1}{\xi^2-\eta^2}\right)|\frac{\partial A_k}{\partial\xi}|^2+\left(\frac{1-\eta^2}{\xi^2-\eta^2}\right)|\frac{\partial A_k}{\partial\eta}|^2}{a^2\int_{\Omega'}K_{11}|A_k|^2} \qquad \cdots \text{ Last term in numerator is positive} \\
&\geq \inf\frac{\int_{\Omega'}\left(\frac{\xi^2-1}{\xi^2-\eta^2}\right)|\frac{\partial A}{\partial\xi}|^2+\left(\frac{1-\eta^2}{\xi^2-\eta^2}\right)|\frac{\partial A}{\partial\eta}|^2}{a^2\int_{\Omega'}K_{11}|A|^2} \\
&\geq R_{00}^2
\end{aligned}$$

Thus we need to look at β with no higher Fourier expansion than zeroth order, i.e. we look for $\beta(\xi, \eta, \theta) = A(\xi, \eta)$.

In prolate spheroidal coordinates the solutions thus are combinations of spheroidal harmonics given by,

$$A(\xi, \eta) = S_{0n}(c, \eta) R_{0n}(c, \xi)$$

Here n gives the ordering of the harmonics, w.r.t. eigenvalues of the spheroidal wave equation λ_{0n}(refer [Fla57] for more on spheroidal wave equation) and c is given by the Neumann boundary condition, i.e.

$$\frac{\partial R_{0n}(c, \xi)}{\partial \xi}(\xi_0)|_{\xi=\xi_0} = 0 \tag{5.37}$$

where $\xi = \xi_0$ is the equation for the surface of the prolate spheroid. To minimize among these solutions, we choose $n = 1$, and choose c as the smallest zero of the boundary condition eqn.(5.37).

5.5.1 Upper Bound for R_{cr}

For upper bound we substitute test functions for $(\beta, \gamma, \mathbf{v})$ in the Rayleigh quotient corresponding to the problem. We choose test functions corresponding to the curling mode.The curling mode was first proposed for the nucleation problem in micromagnetics by W.F.Brown [Bro57] for ferromagnetic domains which are spheres or infinite cylinders. Aharoni [Aha63] gave a characterization of the curling eigenvalue for ferromagnetic prolate spheroids.
$\beta(\xi, \eta, \theta) = R_{11}^{(1)}(c, \xi) S_{11}^{(1)}(c, \eta) \sin\theta = A(\xi, \eta, c) \sin\theta$
$\gamma(\xi, \eta, \theta) = -R_{11}^{(1)}(c, \xi) S_{11}^{(1)}(c, \eta) \cos\theta = -A(\xi, \eta, c) \cos\theta$
$\mathbf{v} = \mathbf{0}$
$\mathbf{m}_0 = (\beta_0, \gamma_0, 0)$

Figure 5.3 gives a snapshot of the eigenvalue across some cross-section of the ellipsoid. Using coordinate relations between Prolate Spheroidal and Cartesian system we transform $\mathbf{m}_0$ to,

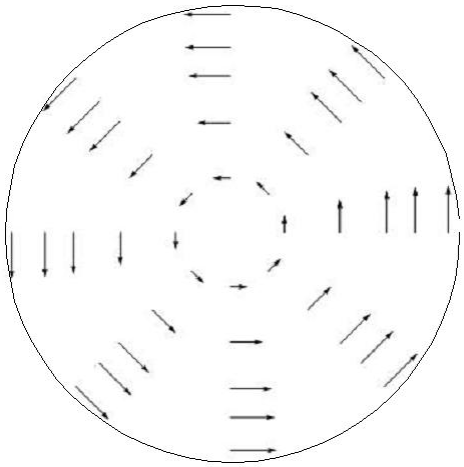

Figure 5.3: Curling mode shown used for upper bound

$$\begin{aligned}
\mathbf{m}_0 &= \Big[-\eta\frac{\sqrt{\xi^2-1}}{\sqrt{\xi^2-\eta^2}}\{A(\xi,\eta,c)\sin\theta\}\cos\theta + (-\eta)\frac{\sqrt{\xi^2-1}}{\sqrt{\xi^2-\eta^2}}\{-A(\xi,\eta,c)\cos\theta\}\sin\theta\Big]\hat{e}_\eta \\
&+ \Big[\xi\frac{\sqrt{1-\eta^2}}{\sqrt{\xi^2-\eta^2}}\cos\theta\{A(\xi,\eta,c)\sin\theta\} + \xi\frac{\sqrt{1-\eta^2}}{\sqrt{\xi^2-\eta^2}}\sin\theta\{-A(\xi,\eta,c)\cos\theta\}\Big]\hat{e}_\xi \\
&- \Big[\{A(\xi,\eta,c)\sin\theta\}\sin\theta - \{-A(\xi,\eta,c)\sin\theta\}\cos\theta\Big]\hat{e}_\theta \\
&= -A(\xi,\eta,c)\hat{e}_\theta \qquad (5.38)
\end{aligned}$$

Note that,

$$\int_\Omega c|\nabla\beta_0|^2 = \int_\Omega c|\nabla\gamma_0|^2 = P$$

$$\int_\Omega |\beta_0|^2 = \int_\Omega |\gamma_0|^2 = Q$$

$$\nabla.\mathbf{m}_0 = \frac{8}{d^3(\xi^2-\eta^2)}\Big[-\frac{\partial}{\partial\theta^2}A(\xi,\eta,c)\Big] = 0$$

$$\mathbf{m}_0.n = \mathbf{m}_0.\hat{e}_\xi = -A(\xi,\eta,c)\hat{e}_\theta.\hat{e}_\xi = 0$$

Thus, $\mathbf{N}(\beta_0,\gamma_0) = 0$.

Thus, using this test functions, we get, upper bound $R_{(ub)}$,

$$
\begin{aligned}
R_{ub}^2 &= \frac{\displaystyle\int_\Omega c(|\nabla\beta_0|^2 + |\nabla\gamma_0|^2)\, d\mathbf{x}}{\displaystyle\int_\Omega -\begin{bmatrix}\beta_0\\ \gamma_0\end{bmatrix}\cdot\mathbf{K}\begin{bmatrix}\beta_0\\ \gamma_0\end{bmatrix} - \mathbf{N}(\beta_\mathbf{0},\gamma_\mathbf{0}) - \mathbf{C}\big[\mathbf{E_s'Wm_0}\big] : \mathbf{E_s'Wm_0} + \mathbf{C}\big[\mathbf{E_v}\big] : \mathbf{E_s'Wm_0}\,\mathbf{dx}} \\
&= \frac{2cP}{2K_1Q - K_1Q - \mathbf{C}\big[\mathbf{E_s'Wm_0}\big] : \mathbf{E_s'Wm_0}} \\
&= \frac{2cP}{K_1Q - \mathbf{C}\big[\mathbf{E_s'Wm_0}\big] : \mathbf{E_s'Wm_0}}
\end{aligned}
\tag{5.39}
$$

Table 5.1 shows numerically computed values for the upper and lower bounds evaluated for different aspect ratios as per the theoretical bounds calculated in this and previous section. As can be seen for larger aspect ratios the lower bounds actually converge to 0 and thus are not very useful. However as mentioned in the previous section, we still get a positive lower bound. The upper bounds calculated in this section changes very slowly with the aspect ratio.

Table 5.1: Lower and upper bound radius for different aspect ratios

anisotropy constant $\times 10^3$ ergs/cc	staturation magnetization emu	exchange constant erg/cm	aspect ratio	R_{lb} nm.	R_{ub} nm.
300	1200	1.8×10^{-6}	2	8	14
300	1200	1.8×10^{-6}	5	4.2	21
300	1200	1.8×10^{-6}	10	3.2	33
300	1200	1.8×10^{-6}	20	3	43
300	1200	1.8×10^{-6}	50	1	44

Chapter 6

Numerical Simulation

6.1 Introduction

To solve for the critical radius we have use the strong form of the equation for the bifurcation modes.

$$c\Delta\beta = R_{cr}^2\Big[(2K_1 + N_z m_s^2) - m_s^2 h_{1_1} - \mathbb{C}[\boldsymbol{E}_v - \boldsymbol{E}_s'\boldsymbol{W}\boldsymbol{m}_0] : \boldsymbol{E}_{s_1}'\Big], \tag{6.1}$$

$$c\Delta\beta = R_{cr}^2\Big[(-K_1 + N_z m_s^2) - m_s^2 h_{1_2} - \mathbb{C}[\boldsymbol{E}_v - \boldsymbol{E}_s'\boldsymbol{W}\boldsymbol{m}_0] : \boldsymbol{E}_{s_2}'\Big], \tag{6.2}$$

with $\boldsymbol{v}$ minimizing for given $\boldsymbol{E}_s'\boldsymbol{W}\boldsymbol{m}_0$,

$$E_{elastic} = \inf_{\boldsymbol{w}\in H^1(\Omega,\mathbb{R}^3)} \int_\Omega \frac{1}{2}\mathbb{C}\big[\boldsymbol{E}_v - \boldsymbol{E}_s'\boldsymbol{W}\boldsymbol{m}_0\big] : (\boldsymbol{E}_v - \boldsymbol{E}_s'\boldsymbol{W}\boldsymbol{m}_0)\, d\boldsymbol{x}\ . \tag{6.3}$$

If we choose $\boldsymbol{v} \equiv 0$ in the above minimization, we get an upper bound for $E_{elastic}$ i.e. $E_{elastic} \le E_{el}^{ub}$ with $E_{el}^{ub} = \mathbb{C}\big[\boldsymbol{E}_s'\boldsymbol{W}\boldsymbol{m}_0\big] : \boldsymbol{E}_s'\boldsymbol{W}\boldsymbol{m}_0$. If we solve the above equations after substituting this upper bound we will get an upper bound for critical radius. For the demagnetization field in the above equations, we use the formula,

$$u(\boldsymbol{x}) = \int_\Omega \nabla_y\Big(\frac{1}{|\boldsymbol{x}-\boldsymbol{y}|}\Big)\cdot \boldsymbol{m}(\boldsymbol{y})\, d\boldsymbol{y}\ . \tag{6.4}$$

$$\boldsymbol{h_m}(\boldsymbol{x}) = -\nabla u(\boldsymbol{x}) = -\nabla_x \int_\Omega \nabla_y\Big(\frac{1}{|\boldsymbol{x}-\boldsymbol{y}|}\Big)\cdot \boldsymbol{m}(\boldsymbol{y})\, d\boldsymbol{y}\ . \tag{6.5}$$

The formula above, gives the solution to Maxwell's equation in distributional sense:

$$\int_{\mathbb{R}^3} \boldsymbol{h_m} \cdot \nabla\phi \, \boldsymbol{dy} = -4\pi \int_{\mathbb{R}^3} \boldsymbol{m}\chi_\Omega \cdot \nabla\phi \, \boldsymbol{dy}, \qquad \forall \phi \in \mathcal{D}(\mathbb{R}^3, \mathbb{R}^3) \ .$$

Note that $\nabla_x \cdot \Big(\frac{1}{|\boldsymbol{x}-\boldsymbol{y}|}\Big) = \nabla_y \cdot \Big(\frac{1}{|\boldsymbol{x}-\boldsymbol{y}|}\Big)$. Using this we see that if $\boldsymbol{m}\chi_\Omega \in L^2(\Omega, \mathbb{R}^3)$, then formula for $\boldsymbol{h_m}$ gives,

$$\begin{aligned}
\boldsymbol{h_m}(\boldsymbol{x}) &= -\nabla_x \int_\Omega \nabla_y \Big(\frac{1}{|\boldsymbol{x}-\boldsymbol{y}|}\Big) \cdot \boldsymbol{m}(\boldsymbol{y}) \, \boldsymbol{dy} \\
&= -\nabla_x \int_\Omega \nabla_x \Big(\frac{1}{|\boldsymbol{x}-\boldsymbol{y}|}\Big) \cdot \boldsymbol{m}(\boldsymbol{y}) \, \boldsymbol{dy} \\
&= -\nabla_x^2 \int_\Omega \Big(\frac{1}{|\boldsymbol{x}-\boldsymbol{y}|}\Big) \boldsymbol{m}(\boldsymbol{y}) \, \boldsymbol{dy} \\
&= -\nabla_x^2 \int_{\mathbb{R}^3} \Big(\frac{1}{|\boldsymbol{x}-\boldsymbol{y}|}\Big) \boldsymbol{m}\chi_\Omega(\boldsymbol{y}) \, \boldsymbol{dy} \\
&= -D_{ij} \int_{\mathbb{R}^3} \Big(\frac{1}{|\boldsymbol{x}-\boldsymbol{y}|}\Big) \boldsymbol{m}\chi_\Omega(\boldsymbol{y}) \, \boldsymbol{dy} \\
&= -D_{ij} 4\pi N(\boldsymbol{m}\chi_\Omega). \qquad (6.6)
\end{aligned}$$

Here $N(\boldsymbol{m}\chi_\Omega)$ is the newtonian potential of $\boldsymbol{m}\chi_\Omega$ given by the convolution $N(\boldsymbol{m}\chi_\Omega)(\boldsymbol{x}) = \dfrac{1}{4\pi|\boldsymbol{x}|} \star \boldsymbol{m}\chi_\Omega(\boldsymbol{x})$. Standard L^p-estimates from reference [GT01] gives us that, T is an operator of strong type (p,p). So for $p=2$,

$$\|D_{ij} N(\boldsymbol{m}\chi_\Omega)\|_{L^2(\mathbb{R}^3)} = \|\boldsymbol{h_m}\|_{L^2(\mathbb{R}^3)} =\leq C\|\boldsymbol{m}\chi_\Omega\|_{L^2(\mathbb{R}^3)} = C\|\boldsymbol{m}\|_{L^2(\Omega)} \ .$$

To check that it solves Maxwell's eqn, note that for all test functions $\phi \in \mathcal{D}(\mathbb{R}^3, \mathbb{R}^3)$,

$$\begin{aligned}
\int_{\mathbb{R}^3} \boldsymbol{h_m}(\boldsymbol{x}) \cdot \nabla\phi(\boldsymbol{x}) \, \boldsymbol{dx} &= \int_{\mathbb{R}^3}\int_{\mathbb{R}^3} -\nabla_x^2 \Big(\frac{1}{|\boldsymbol{x}-\boldsymbol{y}|}\Big) \boldsymbol{m}(\boldsymbol{y})\chi_\Omega \cdot \nabla\phi(\boldsymbol{x}) \, \boldsymbol{dydx}, \\
&= \int_{\mathbb{R}^3}\int_{\mathbb{R}^3} -D_{ij} \Big(\frac{1}{|\boldsymbol{x}-\boldsymbol{y}|}\Big) m_j(\boldsymbol{y})\chi_\Omega \phi_{,i}(\boldsymbol{x}) \, \boldsymbol{dydx}, \\
&= \int_{\mathbb{R}^3} m_j(\boldsymbol{y}) \, \boldsymbol{dy} \chi_\Omega \int_{\mathbb{R}^3} -D_{ij} \Big(\frac{1}{\boldsymbol{x}-\boldsymbol{y}|}\Big) \phi_{,i}(\boldsymbol{x}) \, \boldsymbol{dx} \ .
\end{aligned}$$

Integrating by parts twice the inner integral we have,

$$\begin{aligned}
\int_{\mathbb{R}^3} \boldsymbol{h_m}(\boldsymbol{x}) \cdot \nabla\phi(\boldsymbol{x}) \, \boldsymbol{dx} &= \int_{\mathbb{R}^3} m_j(\boldsymbol{y})\chi_\Omega \, \boldsymbol{dy} \int_{\mathbb{R}^3} -\Big(\frac{1}{|\boldsymbol{x}-\boldsymbol{y}|}\Big) \phi_{,iij}(\boldsymbol{x}) \, \boldsymbol{dx}, \\
&= \int_{\mathbb{R}^3} m_j(\boldsymbol{y})\chi_\Omega \, \boldsymbol{dy} \int_{\mathbb{R}^3} -\Big(\frac{1}{|\boldsymbol{x}-\boldsymbol{y}|}\Big) \Delta\phi_{,j}(\boldsymbol{x}) \, \boldsymbol{dx}, \\
&= -4\pi \int_{\mathbb{R}^3} m_j(\boldsymbol{y})\chi_\Omega \phi_{,j}(\boldsymbol{y}) \, \boldsymbol{dy} \ . \qquad (6.7) \\
&\quad \Big[\quad \because \text{ Newtonian potential of } \Delta\phi_{,j} \text{ is } \phi_{,j} \quad \Big]
\end{aligned}$$

The demag energy is calculated by first numerically integrating for u and then calculating numerical derivative $\boldsymbol{h_m} = -\nabla u$. From Table(3.1) the elastic energy is an order lower in magnitude than anisotropy and magnetostatic energy. So we first neglect the elastic term. The radius calculated thus, will be an lower bound to the actual radius since the elastic energy is a positive energy.

6.2 Mesh and numerical scheme

We use a finite difference technique to solve the equations. The equations are discretized in the prolate spheroidal coordinates. Note that the equations in prolate spheroidal coordinates have singularities along the axis of the ellipsoid given by $\xi = 1, \eta = \pm 1$. To avoid these singularities, we use a staggered mesh thus avoiding both the singularities.

At the points immediately adjoining the singular axis, like points P and Q in Fig.(6.1) we discretize the equations using one side difference formulae (forward or backward depending on point) . At all other mesh points we use central difference. Thus the equation (6.10) becomes a generalized eigenvalue problem for R_1 and the smallest positive eigenvalue R_1 determines the critical radius.

Domain $\Omega(\xi, \eta, \theta) = ([1, \xi_0] \times [-1, 1] \times [0, 2\pi])$.

Mesh points along ξ and η are,
$\xi_i = 1 + (i + 0.5)\delta\xi, \quad i = [1, M]$.
$\eta_j = 1 - (j + 0.5)\delta\eta, \quad j = [1, N]$.

Let S be the total no of mesh points. Vector of nodal values of β, γ is $\boldsymbol{p} = (\beta_1, \beta_2, \cdots, \beta_S, \gamma_1, \gamma_2, \cdots, \gamma_S)^T$. Fig 6.1 shows the mesh in 2-D. Neglecting the elastic energy we get the equations,

$$c\Delta\beta = R_1^2\big[(2K_1 + N_z m_s^2)\beta - m_s^2 h_{1_1}\big] \ . \tag{6.8}$$

$$c\Delta\beta = R_1^2\big[(-K_1 + N_z m_s^2)\gamma - m_s^2 h_{1_2}\big] \ . \tag{6.9}$$

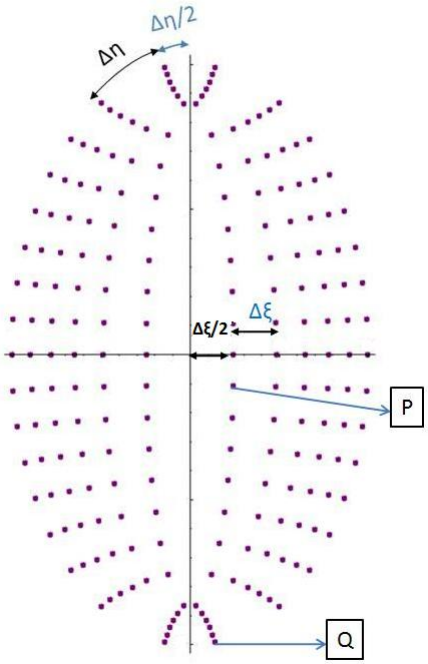

Figure 6.1: Mesh

Discretizing equation (6.5), the demag field vector becomes $\boldsymbol{h}_{1_i} = \boldsymbol{N}_i \boldsymbol{p}$ where $\boldsymbol{N}_i$ is $(S \times 2S)$ matrix and $i = 1, 2$. Discretizing eqn. (6.8),(6.9) we get,

$$L\boldsymbol{p} = \frac{R_1^2}{c}\Big[\boldsymbol{K} - m_s^2 \begin{pmatrix} \boldsymbol{N}_1 \\ \boldsymbol{N}_2 \end{pmatrix}\Big]\boldsymbol{p} \ . \tag{6.10}$$

a. L is discrete form of Laplace operator Δ.

b. $\boldsymbol{K} = \begin{bmatrix} (2K_1 + N_z m_s^2) & 0 \\ 0 & (-K_1 + N_z m_s^2) \end{bmatrix}$

c. $\boldsymbol{N}_i \boldsymbol{p} = \boldsymbol{h}_{1_i} \qquad \cdots i = 1, 2 \qquad \boldsymbol{N}_i$ is $(S \times 2S)$ matrix

6.3 Correction for elastic energy

Let R_1 be the lowest eigenvalue, of (6.10) and $\boldsymbol{p}_1$ be corresponding eigenfunction. Solving (6.10) is equivalent of minimizing the Rayleigh quotient for (6.10). Thus,

$$\frac{R_1^2}{c} = \frac{\boldsymbol{p}_1.L\boldsymbol{p}_1}{\boldsymbol{p}_1.\left[\boldsymbol{K} - \binom{N_1}{N_2}\right].\boldsymbol{p}_1} \ .$$

Here the r.h.s. is the numerical form of the Rayleigh quotient. Now if we include the upper bound to elastic energy E_{el}^{ub} in ratio and evaluate it at the test function $\boldsymbol{p}_1$ we get an upper bound to critical radius. i.e. we set R_2 as,

$$\frac{R_2^2}{c} = \frac{\boldsymbol{p}_1.L\boldsymbol{p}_1}{\boldsymbol{p}_1 \cdot \left[K - \binom{N_1}{N_2} - E_{el}^{ub}(\boldsymbol{p}_1)\right]\boldsymbol{p}_1} \ .$$

The difference between numerically computed values of $R_1 \leq R_{cr} \leq R_2$ for the range in which numerical experiments were conducted was of $\sim 1\%$ and thus does not justify the inclusion of full elastic energy in computing the critical radius.

6.4 Table of results

Table 6.1 shows actual numerical critical radius computed from eqn.(6.10) for few aspect ratios q. In principle numerical computation can be done for higher aspect ratios.

Table 6.1: Critical radius for different aspect ratios

anisotropy constant $\times 10^3$ ergs/cc	staturation magnetization emu	exchange constant erg/cm	aspect ratio	R_{cr} nm.
300	1200	1.8×10^{-6}	2	12
300	1200	1.8×10^{-6}	5	18
300	1200	1.8×10^{-6}	10	26
300	1200	1.8×10^{-6}	20	35

References

[Aha63] A. Aharoni. Complete Eigenvalue Spectrum for the Nucleation in a Ferromagnetic Prolate Spheroid. *Physical Review*, 131(4):1478–1482, 1963.

[Bra02] A. Braides. *Gamma-Convergence for Beginners*. Oxford University Press, 2002.

[Bro57] W.F. Brown. Criterion for Uniform Micromagnetization. *Physical Review*, 105(5):1479–1482, 1957.

[Bro63] W.F. Brown. *Micromagnetics*. Interscience Publishers New York, 1963.

[Bro66] W.F. Brown. *Magnetoelastic Interactions*. Springer-Verlag, 1966.

[CHWF+03] AE Clark, KB Hathaway, M. Wun-Fogle, JB Restorff, TA Lograsso, VM Keppens, G. Petculescu, and RA Taylor. Extraordinary magnetoelasticity and lattice softening in bcc Fe-Ga alloys. *Journal of Applied Physics*, 93:8621, 2003.

[CK98] R. Choksi and R.V. Kohn. Bounds on the micromagnetic energy of a uniaxial ferromagnet. *Communications on Pure and Applied Mathematics*, 51(3):259–289, 1998.

[CRWF+00] AE Clark, JB Restorff, M. Wun-Fogle, TA Lograsso, DL Schlagel, C. Associates, and MD Adelphi. Magnetostrictive properties of body-centered cubic Fe-Ga andFe-Ga-Al alloys. *IEEE Transactions on Magnetics*, 36(5 Part 1):3238–3240, 2000.

[Dac89] B. Dacorogna. *Direct methods in the calculus of variations*. Springer-Verlag New York, Inc. New York, NY, USA, 1989.

[DFMS08] P.R. Downey, A.B. Flatau, P.D. McGary, and B.J.H. Stadler. Effect of magnetic field on the mechanical properties of magnetostrictive iron-gallium nanowires. *Journal of Applied Physics*, 103:07D305, 2008.

[DS93] A. De Simone. Energy minimisers for large ferromagnetic bodies, Arch. *Rational Mech. Anal*, 125:99, 1993.

[Fla57] C. Flammer. *Spheroidal wave functions*. Stanford University Press Stanford, Calif, 1957.

[Gra91] K.F. Graff. *Wave motion in elastic solids*. Dover Pubns, 1991.

[GT01] D. Gilbarg and N.S. Trudinger. *Elliptic Partial Differential Equations of Second Order*. Springer, 2001.

[IKO+02] O. Ikeda, R. Kainuma, I. Ohnuma, K. Fukamichi, and K. Ishida. Phase equilibria and stability of ordered bcc phases in the Fe-rich portion of the Fe–Ga system. *Journal of Alloys and Compounds*, 347(1-2):198–205, 2002.

[LL35] L. Landau and E. Lifshitz. On the theory of the dispersion of magnetic permeability in ferromagnetic bodies. *Physik. Z. Sowjetunion*, 8:153–169, 1935.

[PHL+05] G. Petculescu, KB Hathaway, TA Lograsso, M. Wun-Fogle, and AE Clark. Magnetic field dependence of galfenol elastic properties. *Journal of Applied Physics*, 97:10M315, 2005.

[RCWC04] S. Rafique, J.R. Cullen, M. Wuttig, and J. Cui. Magnetic anisotropy of FeGa alloys. *Journal of Applied Physics*, 95:6939, 2004.

[SB88] M.E. Schabes and H.N. Bertram. Magnetization processes in ferromagnetic cubes. *Journal of Applied Physics*, 64:1347, 1988.

Appendix A

Magnetostatic energy

The Maxwell's equation in the absence of current, gives the relation for the self energy of a ferromagnetic body $\Omega \subset \mathbb{R}^3$. The equations are given by,

$$\begin{cases} \nabla \times \boldsymbol{h_m}(\boldsymbol{x}) = 0 \qquad \boldsymbol{x} \in \mathbb{R}^3 \\ \nabla \cdot \big(\boldsymbol{h_m}(\boldsymbol{x}) + 4\pi \boldsymbol{m}(\boldsymbol{x})\chi_\Omega\big) = 0 \qquad \boldsymbol{x} \in \mathbb{R}^3 \end{cases}$$

Here, $\boldsymbol{m}$ is the given magnetization vector on the body Ω, and $\boldsymbol{m}\chi_\Omega$ is the magnetization extended outside the body to all space by 0. The solution $\boldsymbol{h_m}$ is understood to satisfy the above in the sense of distributions, as in the general case, if $\boldsymbol{m} \in L^2(\Omega, \mathbb{R}^3$, then $\nabla \cdot \boldsymbol{m}\chi_\Omega$ is not even a function but rather a distribution. The first equation means that $\boldsymbol{h_m} = -\nabla u$ for some $u \in H^1(\mathbb{R}^3)$. Thus if $\boldsymbol{m} \in W^{1,2}(\Omega, \mathbb{R}^3)$ then the above equations imply,

$$\begin{cases} \boldsymbol{h_m} = -\nabla u & \text{in } \mathbb{R}^3 \\ \Delta u = 4\pi \nabla \cdot \boldsymbol{m} & \text{in } \Omega \\ \Delta u = 0 & \text{in } \mathbb{R}^3/\Omega \\ [|-\nabla u \cdot \boldsymbol{n}|] = \boldsymbol{m} \cdot \boldsymbol{n} & \text{on } \partial\Omega \end{cases}$$

In the distributional sense these equations imply,

$$\int_{\mathbb{R}^3} \nabla u \cdot \nabla v \, \boldsymbol{dx} = 4\pi \int_{\mathbb{R}^3} \boldsymbol{m}\chi_\Omega \cdot \nabla v \, \boldsymbol{dx}, \qquad \forall v \in H^1(\mathbb{R}^3) \ .$$

The Lax-Milgram theorem gives existence and uniqueness for above problem. The representation form of the solution used in the last section can be seen by using Fourier transform. The magnetostatic energy of the magnetized body is given by, $\int_{\mathbb{R}^3} |\boldsymbol{h_m}|^2$. In the distributional form of the equation if we choose the test function $v = u$ we get,

$$\int_{\mathbb{R}^3} |\boldsymbol{h_m}|^2 = \int_{\mathbb{R}^3} \nabla u \cdot \nabla u = 4\pi \int_{\mathbb{R}^3} \boldsymbol{m}\chi_\Omega \cdot \nabla u = -4\pi \int_\Omega \boldsymbol{m} \cdot \boldsymbol{h_m} \ .$$

Taking Fourier transform of Maxwell's equation we get,$-|\boldsymbol{\xi}|^2 \hat{u}(\boldsymbol{\xi}) = -4\pi i \boldsymbol{\xi} \cdot \hat{\boldsymbol{m}}$.

$$\hat{\nabla u}(\boldsymbol{\xi}) = i\boldsymbol{\xi}\hat{u}(\boldsymbol{\xi}) = -4\pi i^2 \boldsymbol{\xi}\Big(\frac{\boldsymbol{\xi} \cdot \hat{\boldsymbol{m}}}{|\boldsymbol{\xi}|^2}\Big) = 4\pi \frac{(\boldsymbol{\xi} \otimes \boldsymbol{\xi})\hat{\boldsymbol{m}}}{|\boldsymbol{\xi}|^2} \ .$$

To see the representation form for solution used in the previous section on Numerical results we note that we can take inverse transform of $\hat{\nabla u}$ using convolution theorem, to get,

$$\boldsymbol{h_m}(\boldsymbol{x}) = \int_{\mathbb{R}^3} \nabla^2 N(\boldsymbol{x} - \boldsymbol{y})\boldsymbol{m}(\boldsymbol{y})\, dy, \text{ where } N(\boldsymbol{x}) = \frac{1}{|\boldsymbol{x}|} \ .$$

The above form for $\boldsymbol{h_m}$ makes sense in light of standard L^p-estimates and the Calderon-Zygmund type inequality. An interesting property of the above equations is that for ellipsoidal domains when $\boldsymbol{m}$ is constant over the domain, the demag field, $\boldsymbol{h_m}$ is also constant. For such domains,

$$\boldsymbol{h_m}(\boldsymbol{x}) = 4\pi \boldsymbol{D}\boldsymbol{m}(\boldsymbol{x}) \qquad\qquad \forall \boldsymbol{x} \in \Omega \ .$$

. Here $\boldsymbol{D}$ is a constant symmetric matrix independent of $\boldsymbol{x}$ and it has Trace($\boldsymbol{D}$) = 1. For all domains of finite volume, $\boldsymbol{D}$ is positive definite. Given $\boldsymbol{D}$ is symmetric and positive definite, it can be diagonalized. For very long thin prolate ellipsoids with aspect raio $p > 1$, the form for $\boldsymbol{D}$ is,

$$\boldsymbol{D} = \begin{bmatrix} \frac{1}{2} - \alpha & 0 & 0 \\ 0 & \frac{1}{2} - \alpha & 0 \\ 0 & 0 & 2\alpha \end{bmatrix}, \text{ where } \alpha = \frac{1}{2(p^2-1)}\Big[\frac{p}{\sqrt{p^2-1}} \ln(p + \sqrt{p^2-1}) - 1\Big] \ .$$

Here the coordinate system used for D represent the 3 axis of the ellipsoid with the z-axis lying along the long axis and corresponding to the eigenvalue α and x,y axis corresponding to $\frac{1}{2} - \alpha$.